

MOLECULAR WEIGHT DETERMINATION OF POLYSACCHARIDES

Stephen E. Harding, Kjell M. Vårum, Bjørn T. Stokke
and Olav Smidsrød

OUTLINE

1. Introduction: Why Measure Polysaccharide Molecular Weight?	64
2. Why is Polysaccharide Molecular Weight Determination Difficult?	69
2.1 Heterogeneity and Polydispersity	69
2.2 Thermodynamic Non-ideality	72
2.3 Concentration Measurement	73
3. Osmosis	74
3.1 General Background	75
4. Static Light Scattering	82
4.1 General Background	82
4.2 Polyelectrolytes	87
4.3 Clarification of Solutions	88

Advances in Carbohydrate Analysis
Volume 1, pages 63–144
Copyright © 1991 JAI Press Ltd
All rights of reproduction in any form reserved.
ISBN: 1-55938-265-1

5. Sedimentation Equilibrium	90
5.1 Some Basic Theory	91
5.2 Low Speed Versus High Speed Sedimentation Equilibrium	95
5.3 Sedimentation Equilibrium and Thermodynamic Non-ideality	96
5.4 Polydispersity Versus Self-association Phenomena	98
5.5 Other Advances in Theory and Methodology	100
5.6 Applications	101
6. Relative Techniques	103
6.1 Viscometry	103
6.2 Sedimentation Velocity	111
6.3 Translational Diffusion Coefficient Determination: Dynamic Light Scattering	113
7. Gel Permeation Chromatography	116
7.1 Selection of Column Material	118
7.2 Calibration using Standards	120
7.3 Calibration for System Dispersion	124
8. Maxwell's Demon: Combined Fractionation/Absolute Approaches	125
8.1 Off-line Calibration of Gel Permeation Chromatography by Sedimentation Equilibrium	127
8.2 Off-line Calibration of Gel Permeation Chromatography by Total Intensity Light Scattering	127
8.3 On-line Calibration of Gel Permeation Chromatography by Low Angle Laser Light Scattering	129
8.4 On-line Calibration of Gel Permeation Chromatography by Multi-angle Laser Light Scattering	129
8.5 On-line SFFF/Light Scattering	131
9. Other Methods	132
10. Conclusions	135
References	138

1. INTRODUCTION: WHY MEASURE POLYSACCHARIDE MOLECULAR WEIGHT?

One of the most fundamental parameters characterizing a macromolecule—whether it be naturally occurring or synthetically

produced—is its ‘molecular weight’ or ‘relative molecular mass’. The former term is preferred when the parameter is used in a thermodynamic sense since it is not a dimensionless quantity but has defined units: g/mol in the c.g.s. system. Despite the fundamental nature of this parameter, for certain classes of macromolecules—including polysaccharides—it has proved very difficult to determine. In the case of polysaccharides this is principally because of four basic properties:

- (a) They are polydisperse, that is consist of species of different molecular weight
- (b) They are highly non-ideal in the thermodynamic sense. This high non-ideality can arise from two sources: (i) high thermodynamic exclusion volumes resulting from large assymmetry or high solvent affinity and (ii) polyelectrolyte behaviour.
- (c) Unlike globular proteins they can have a conformation in solution that is difficult to define or determine with any precision. This can seriously affect the accuracy of those techniques which require assumptions to be made about the conformation in solution for obtaining molecular weights.
- (d) A further complication is that some polysaccharides self-associate, particularly at higher solute concentrations.

Indeed, it is fair to say that a single determination of an average molecular weight or even more so, a molecular weight distribution, of any new polysaccharide preparation can still require a research project of some difficulty and duration. These difficulties are unfortunate since knowledge of the molecular weights of polysaccharides is in general of fundamental importance for the understanding of their biotechnological applications and their role in living systems as we know them today. Such knowledge is important also in a large number of medical and commercial applications [1] as detailed in the following paragraphs.

Application in the food industry. The performance of pectins and alginates as gelling and thickening agents is diminished by the presence of ‘low molecular weight tails’ in the molecular weight distribution (see, e.g. Launay *et al.* [2]). Another example of the tail wagging the dog is the current concern of possible toxicity of low molecular weight forms of carrageenan (see, e.g. Engster and Abraham [3])—this product has been banned from food products in certain countries.

The oil industry. Polysaccharides have found their way into the oil industry mainly as additives to drilling muds—to prevent fluid loss, for suspending particles and for rheological control—and as additives to injected fluids for mobility control to improve sweep efficiency in flooding operations. The effectiveness of a polysaccharide for mobility control is to a large extent determined by its molecular weight [4].

Pharmaceutical applications. Polysaccharides are increasingly being used in drug delivery systems, both as carrier systems for (intravenous) drug targeting [5], for increasing the transit time of novel dosage forms in the small intestine [6] and controlled release forms [7]. In all three cases the performance of the delivery system is closely related to the transport properties of the carrier system which depends, amongst other factors, on the molecular weight of polysaccharide vaccines [8].

Medical applications. For any use of polysaccharides in medicine (dextrans, schizophyllan, hyaluronic acid, heparin, chondroitin sulphate, chitosan, etc.) the applied or injected systems should, in addition to having some specific physiological properties depending on the chemical structure of the polymer, confine within a narrow set of values for physical properties like osmotic pressure, viscosity, gel or fibre properties, etc.; all properties critically dependent on molecular weight and molecular weight distributions. The specific medical response may also be molecular weight dependent as suggested for the immune stimulatory effect of schizophyllan where the existence of the triple helix, stable only above a certain molecular weight, is the basis for the immune response [9].

Biological significance of molecular weight. Hyaluronic acid, which is a major constituent of the synovial fluid in all our joints, is responsible for the rheological control of such fluids. It is remarkable that the friction coefficient in our knees is lower than that of most man made machines [10]. Both the molecular weight and the concentration level of hyaluronic acid is crucial for the proper lubrication of joints [10]. As the viscoelastic properties are strongly dependent on the molecular weight in the concentration range found in synovial fluids (2.2–2.4 mg/ml), changes in molecular weight strongly affect the rheological properties and thereby lubrication properties of such fluids.

The performance of polysaccharides in other applications is also influenced by their molecular weights. For example, in the wood pulp/paper industry there has been an extensive literature on the determination of molecular weight distributions of cellulose and cellulose derivatives, largely using gel permeation chromatography [11]. Other examples include the performance of polysaccharides in shampoo [12], paint [13] and wine. There are now several techniques—some independent, some not—at our disposal for polysaccharide molecular weight analysis and in Table 1 we have cited the most important of these. They have been classified into either 'absolute', 'relative' or 'combined'. Absolute techniques such as membrane osmometry, 'static' light scattering or sedimentation equilibrium require no assumptions about macromolecular conformation and do not require calibration using standards of known molecular weight. Relative techniques, such as gel permeation chromatography, sedimentation velocity, dynamic light scattering and viscometry require either knowledge/assumptions concerning macromolecular conformation or calibration using so-called 'standard' polysaccharides (commonly dextrans or pullulans). Absolute molecular weights can also be obtained by combining information from two or more 'relative' techniques, for example sedimentation velocity with dynamic light scattering (diffusion coefficient) measurements (Svedberg equation—see, e.g. Tanford [14]) or sedimentation velocity with intrinsic viscosity (Scheraga–Mandelkern equation [14–16]) although the latter still requires the use of a parameter (β) which is taken for the purpose of molecular weight measurement as insensitive to shape.

Off-line and on-line combined approaches for obtaining absolute molecular weight distributions directly and molecular weight averages indirectly, from conservation-of-mass type calculations based on the form of these calculated distributions, are becoming increasingly popular (Table 1) and these are based on either one of two relative techniques: gel permeation chromatography (GPC) or a particular type of sedimentation velocity technique known as sedimentation field flow fractionation (SFFF). An absolute molecular weight method is used to give either off-line calibration of GPC [static light scattering (SLS), or sedimentation equilibrium], on-line calibration of GPC [low angle SLS, conventional (multi-angle) SLS and viscometry (the latter assuming the validity of a universal

Table 1. Molecular weight averages from different techniques.

Method	Type of average	Scaling parameters				Scaling relation
		Rod configuration	Random coil Good	Compact sphere	Theta	
1. Absolute techniques						
Osmotic pressure	$\langle M_{w,1} \rangle = M_n$					
Classical Light scattering	$\langle M_{1,0} \rangle = M_w$					
Sedimentation equilibrium	$\langle M_{1,0} \rangle = M_w$					
	(M_n, M_w, M_{v1}, M_{v2})					
2. Relative techniques						
Intrinsic viscosity	$M_\eta = \langle M_{u,0} \rangle$	$a =$	1.8	0.8	0.5	$[\eta] = K'M^a$
Sedimentation velocity	$M_s = \langle M_{u,0} \rangle$	$b =$	0.15	0.4	0.5	$s = K''M^b$
Dynamic light scattering (Diffusion coefficient)	$M_{\text{dif}} = \langle M_{1,1-v} \rangle$	$c =$	1.0	(0.62)	0.5	$D = K'''M^c$
Gel permeation chromatography						Molecular weight distribution = > different types of averages
3. Combined approaches						
Viscosity and sedimentation (Scheraga-Mandelkern)	$M_{\eta,s}$					
Sedimentation velocity and dynamic light scattering	M_w					

calibration curve)] or on-line calibration of SFFF (using a light scattering detector).

It is the primary intention of this review to alert both academics and industrialists alike to the principal techniques available for the determination of polysaccharide molecular weights, and to identify the possibilities and limitations of them; their limitations have sometimes been overlooked in the recent literature. It is not the purpose of this article to give a treatise on the theoretical or experimental details of the techniques: such treatments can be found in the many standard texts and reviews identified in the individual techniques considered in turn below. It would be instructive first, however, to define the problem in terms of heterogeneity, polydispersity and thermodynamic non-ideality.

2. WHY IS POLYSACCHARIDE MOLECULAR WEIGHT DETERMINATION DIFFICULT?

2.1. Heterogeneity and Polydispersity

Polysaccharides are heterogeneous substances. By heterogeneity we mean any deviation from single molecular weight behaviour of a polysaccharide preparation no matter what the cause of the variation may be (Fig. 1 [17]). (Definitions of the terms 'heterogeneity' and 'polydispersity' vary in the literature: thus our use here differs from that of Gibbons [17].) One contribution will be from 'polydispersity', i.e. the presence of non-interacting components of different molecular weight or composition. This can arise from two causes: a quasi-continuous variation in the lengths/weights of individual polysaccharide macromolecules ('primary polydispersity')—which affects all polysaccharides—or from the presence of discrete components of different molecular weights/compositions ('secondary polydispersity')—the latter applies to polysaccharide preparations containing mixtures of polysaccharides. A second contribution to sample heterogeneity can arise from potential self-association phenomena e.g. with guar [18].

The molecular weight heterogeneity of polysaccharides can be described by several types of average molecular weight. The principal molecular weight averages are: number average, weight average and z-average. For an ensemble of macromolecules with n_i

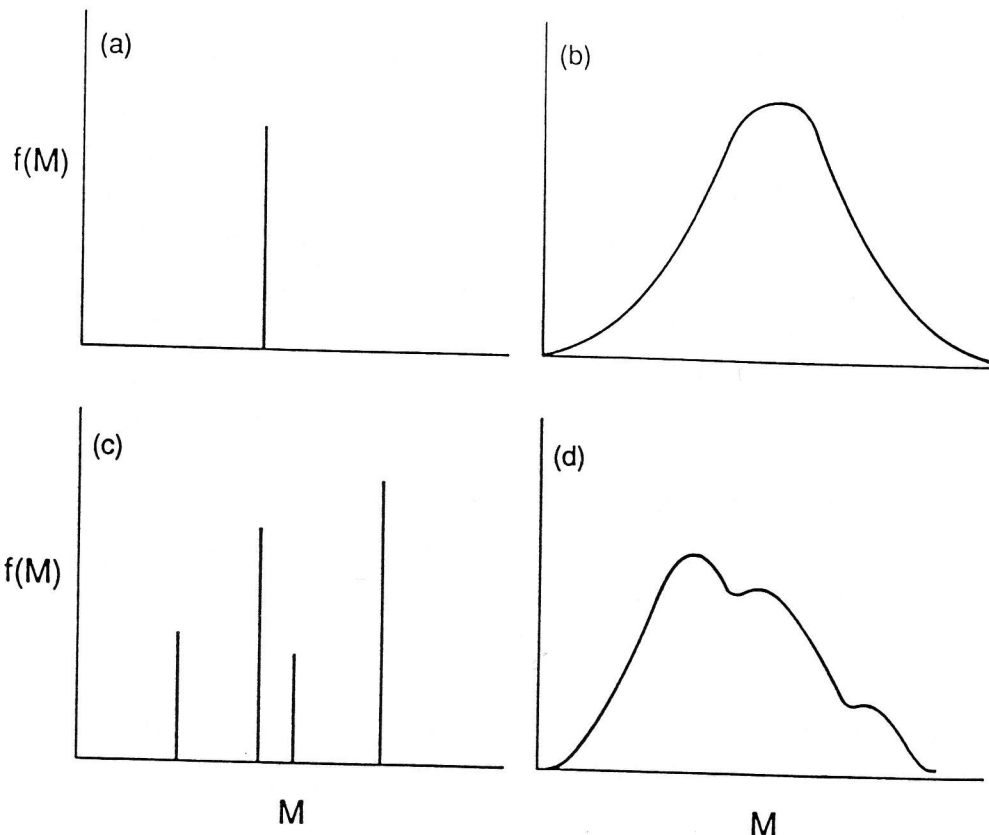


Figure 1. Types of Polydispersity. (a) Monodisperse. (b) Quasi-continuous ('primary' polydispersity). (c) Discrete ('secondary' polydispersity or 'paucidisperse'). (d) Polydisperse mixture. Adapted from Ref. [17].

components whose molecular weights are M_i and whose concentrations are c_i , the number, weight and z-averages are:

$$M_n = \frac{\sum n_i M_i}{\sum n_i} = \frac{\sum c_i}{\sum c_i / M_i} \quad (2.1)$$

$$M_w = \frac{\sum n_i M_i^2}{\sum n_i M_i} = \frac{\sum c_i M_i}{\sum c_i} \quad (2.2)$$

$$M_z = \frac{\sum n_i M_i^3}{\sum n_i M_i^2} = \frac{\sum c_i M_i^2}{\sum c_i M_i} \quad (2.3)$$

Alternatively, these principal averages can be expressed in terms of the general formulation, where k is an integer [19]:

$$\langle M_{k+1,k} \rangle = \frac{\sum c_i M_i^{k+1}}{\sum c_i M_i^k} \quad (2.4)$$

where $\langle M_{0,-1} \rangle = M_n$, $\langle M_{1,0} \rangle = M_w$, and $\langle M_{2,1} \rangle = M_z$. Equation (2.4) can be generalized to non-integer k to include more complex

types of average:

$$\langle M_{\alpha,p} \rangle = \left[\frac{\sum c_i M_i^\alpha}{\sum c_i M_i^p} \right]^{1/(\alpha-p)} \quad (2.5)$$

In this formulation the viscosity average (see later), $M_\eta = \langle M_{\alpha,0} \rangle$ where α is the exponent in the Mark-Houwink-Kuhn-Sakurada equation.

In Table 1 we identify what principal averages the various techniques can provide. For example membrane osmometry is a colligative property, i.e. a function of the *numbers* of molecules, whereas sedimentation equilibrium and light scattering give averages that are principally dependent on the *weight* concentrations of the components and hence yield weight averages. The relative techniques provide a type of molecular weight average that depends on the conformation adopted by the polysaccharide in solution. Table 1 also shows that potential molecular weight resolution depends on the conformation and the particular relative technique chosen: The stronger the molecular weight dependence of the observed property, the better the resolving power. This should be taken into account when selecting a relative method to determine molecular weight.

Polydispersities are in many cases reported as the ratios $I_{pn} = M_w/M_n$, or $I_{pw} = M_z/M_w$, and are often referred to as 'polydispersity indeces' by commercial manufacturers of polysaccharides. Their values can be obtained as estimates from GPC or from absolute methods for determination of molecular weights. These ratios might shed some light on the type of molecular weight distribution, i.e. $I_{pn} > I_{pw}$ for a normal distribution. The ratios provide a useful rule of thumb as to whether the material is 'polydisperse' ($I_p \geq 1.6$) or nearly monodisperse ($I_p \leq 1.1$), but should never be substituted for the characterization of the whole molecular weight distribution.

For polysaccharides that are copolymers or form mixtures of polysaccharides some caution is advised when interpreting ultracentrifuge or (static) light scattering data. This is because of possible polydispersity in the partial specific volume (ultracentrifugation) or specific refractive increment (light scattering) both corresponding to variations in *composition* of a given polysaccharide preparation.

2.2 Thermodynamic Non-ideality

One distinguishing feature of polysaccharides when compared with relatively well behaved macromolecules such as many proteins is that they are very non-ideal in the thermodynamic sense because of their large exclusion volumes and in many cases high charge. Since physical measurements on polysaccharides have to be made at a finite concentration, there will be a contribution from these effects. For example the expression for the osmotic pressure of a solution, correct to first order in the virial coefficient expansion, is [20]:

$$\Pi/c = [RT/M_n](1 + BM_n c) \quad (2.6)$$

where B is the second virial coefficient. Equation (2.6) is normally adequate for polysaccharide solutions of concentrations less than 10 mg/ml, except in extreme cases. Although the equation here refers specifically to osmotic pressure, other similar relations exist for other solution physical measurements, notably static light scattering (Section 4.1) and sedimentation equilibrium (Section 5.1).

Expected ranges of values for the thermodynamic second virial coefficient, B , for various polysaccharide-solvent systems are given in Table 2. In Table 3 [21-31] we have compared the non-ideality parameters, B and BM for several polysaccharides and also included (to demonstrate the orders of magnitude involved) values for a protein (haemoglobin) and a hypothetical unhydrated spherical particle. We have also given values for the term $1 + BMC$ for a weight concentration (c) of 0.4 mg/ml: this term ($1 + BMC$) represents the factor by which the apparent molecular weight is diminished compared with the ideal value. (For sedimentation equilibrium and light scattering the correction factor is $\sim 1 + 2BMC$.) It will be seen that for alginates the

Table 2. Values of B for different polysaccharide-solvent systems.

B (ml mol/g ²)	Type of molecule
Less than 0	any polysaccharide in a poor solvent; self-association of the polysaccharides
~ 0	ideal solvent (θ solvent)
10^{-5} to 10^{-4}	compact spheres
$\sim 10^{-3}$	coils in good solvents, polyelectrolytes

Table 3. Comparative non-ideality of polysaccharides.

Substance	$10^{-6} \times M$ (g/mol)	$10^4 \times B^a$ (ml mol/g ²)	BM (ml/g)	$1 + BMC^b$	Ref.
Sphere, unhydrated ^c	0.50	0.06	3	1.001	21
Haemoglobin	0.064	0.07	4.8	1.002	22
Pullulan P5	0.0053	10.3	5.5	1.002	23
Pullulan P50	0.047	5.5	25.9	1.010	23
Pullulan P800	0.76	2.3	175	1.070	23
Pullulan P1200	1.24	2.2	273	1.109	23
Xanthan (Fraction)	0.36	2.4	86	1.035	23
β -Glucan	0.17	6.1	104	1.042	24
Dextran T-500	0.42	3.4	143	1.057	25
Chitosan (Protan 203)	0.44	5.1	224	1.090	26
Bacterial (XM6)	2.0	1.3	260	1.104	27
Hyaluronate (hydrolysed)	0.070	4.1	287	1.114	27
Citrus Pectin (Frac)	0.045	50.0	450	1.180	28
Scleroglucan	5.7	0.50	570	1.228	29, 30
Alginate (Laminaria)	0.35	29.0	1015	1.406	31

^a B is the osmotic pressure second virial coefficient (determined by either osmotic pressure directly, sedimentation equilibrium or light scattering).

^bBased on a value for the concentration, c of 0.4 mg/ml.

^cHypothetical spherical particle, $\bar{v} = 0.75$ ml/g.

effects are particularly severe. The reader is referred to Tanford [14] for a more detailed discussion of the variation of the second virial coefficient with the shape and molecular weight of a macromolecule.

2.3 Concentration Measurement

Determination of weight concentrations precisely is not easy for polysaccharides, and this is not always appreciated in the literature: one of the principal contributors to data error is error in concentration. Errors can largely be minimized in sedimentation velocity or diffusion coefficient determinations through 'serial dilution' extrapolations to zero concentration, but will affect the evaluation of partial specific volumes (from the slope of plots of density versus concentration), refractive index increments (from the slope of refractive index versus concentration), static light scattering plots and also evaluations of intrinsic viscosities.

Because most polysaccharides do not absorb in the (usable) UV, concentrations are frequently determined refractometrically [29], or by using specific chemical assays e.g. the phenol-sulphuric acid method for polyuronides [32]). However, all these methods require calibration at some stage using a dry-weight type of evaluation. Correction for moisture content in polysaccharide samples is most frequently done by drying the sample in an exicator until a constant weight is achieved. It is, however, a problem that such samples may be strongly hygroscopic. One alternative is to determine the amount of carbon in the sample by means of an elemental analyser and convert that data to polysaccharide concentration. In our opinion, whatever method is used concentrations can be measured to no better than $\pm 3\text{--}5\%$. A given determination of the molecular weight for a polysaccharide preparation has therefore, for most of the techniques, a rather large uncertainty associated with it due to the uncertainty in the concentration determination. This should always be recognized when evaluating a molecular weight.

3. OSMOSIS

Osmotic pressure measurements are relatively easy to make and, provided care is taken to obtain reliable values, the results can be interpreted with relatively high confidence. The method is the major technique for determining the number-average molecular weight (M_n) of polysaccharides, together with end-group analysis. In addition to determination of the M_n , the method also provides estimation of the osmotic second virial coefficient, which may yield information on the shape, the net charge and possible interactions between the macromolecules. However, the relatively low sensitivity of the method to high molecular weight polysaccharides, as the osmotic pressure at high dilution is sensitive only to the *number* of particles in the solution, will in practice limit its use to polysaccharides with molecular weights of less than 500 000. There is also a lower limit of molecular weight that can be determined by this method, which is related to the type of membrane which is used. The principal requirement for reliable molecular weight determination by osmosis is that the membrane is impermeable to the macromolecules of the lowest molecular weight in the sample.

3.1 General Background

The distribution of diffusible molecules across a semipermeable membrane is governed by the requirement that their chemical potential is equal on both sides of the membrane. We will treat the theory of osmotic pressure for neutral and charged polysaccharides separately. For a more detailed treatment of the theory, the reader is referred to Tanford [14] or Tombs and Peacocke [20].

3.1.1 Neutral Polysaccharides

Consider a situation where the polysaccharide solution is placed on one side of a semipermeable membrane, which is not permeable to the polysaccharide (Fig. 2). The polymer will reduce the chemical potential of its solvent and, because it cannot pass through the membrane, the solvent molecules will tend to 'dilute' the polysaccharide solution by flowing through the membrane from the solvent side until the chemical potential for the diffusible solvent molecules is equal on both sides of the membrane. The initial difference in chemical potential for the solvent over the membrane will be compensated for by a build up of the osmotic pressure, Π .

In dilute solutions (see, e.g. Tanford [14]), it can be shown that the osmotic pressure is related to the weight concentration of polysaccharide, c , through the equation

$$\Pi = RT(c/M_n + Bc^2 + Cc^3 + \dots) \quad (3.1)$$

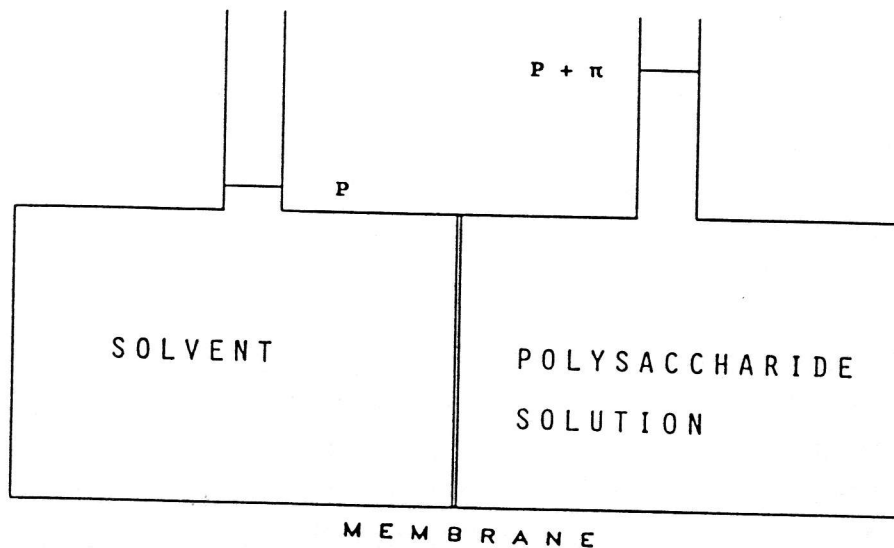


Figure 2. Schematic diagram of an osmometer.

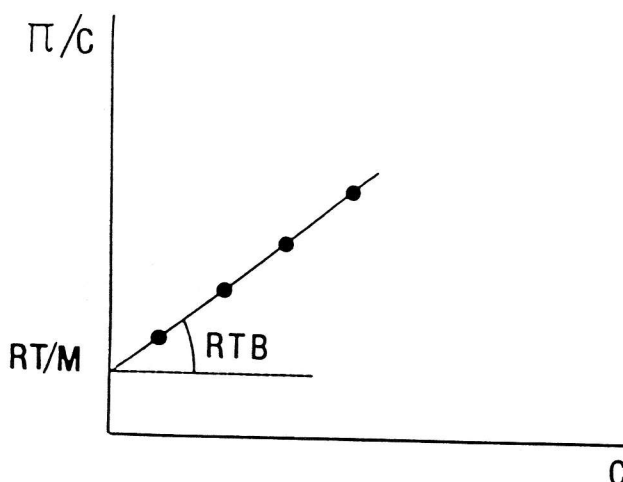


Figure 3. Example of plotting of osmotic pressure data for the determination of M_n and B .

where M_n is the number-average molecular weight of the polysaccharide, R the molar universal gas constant, T the absolute temperature, B the second virial coefficient and C the third virial coefficient. For dilute polymer solutions, it is usually enough to consider the first and second virial coefficient of (3.1), and by dividing by c we get

$$\Pi/c = RT/M_n + RTBc \quad (3.2)$$

Experimentally determined osmotic pressures at different concentrations yields M_n as the intercept of a graph of Π/c versus c (Fig. 3) extrapolated to zero concentration. The slope of such a graph provides a value of the second virial coefficient, B .

3.1.2 Charged Polysaccharides (Polyelectrolytes)

An important effect caused by charged polysaccharides is the distribution of small ions across the semipermeable membrane. In addition to the requirement of identical chemical potential at both sides of the membrane for the diffusible salt, the presence of the polyelectrolyte also adds the zero net electrical charge requirement to the equilibrium situation. Polysaccharides are very often charged, and are accompanied by their corresponding neutralizing counter-ions, but the number of charges can vary from one (or even more) per monosaccharide unit to only a few charges per polymer molecule. We will treat the polyelectrolytes with and without the presence of a salt that can diffuse through the semipermeable membrane.

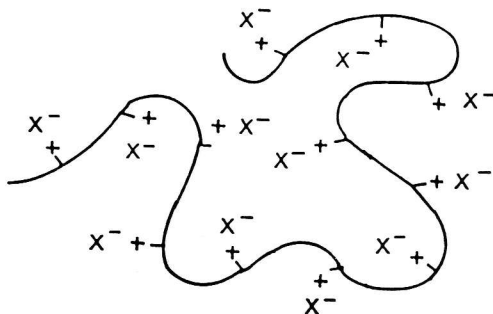


Figure 4. Schematic polyelectrolyte with positive charges.

Without salt. We will consider a polycation, a positively charged polysaccharide (Fig. 4). The results will be analogous for poly-anions for the *co*-ions (salt-ion with the same charge as the polysaccharide) and for the *counter*-ion (salt-ions with the opposite charge of the polysaccharide).

When such a polycation dissolves in water, the counterions will dissociate according to the equation:

$$\text{Pol } X_z = \text{Pol}^{z+} + zX^- \quad (3.3)$$

where Pol is the polymer molecule (with z positive charges) and X is the counterion. Each polymer molecule will dissociate into $(1 + z)$ particles. The counterions will not diffuse freely across the membrane, but are kept at the polymer side of the membrane because of the zero net electrical charge requirement. From (3.2) we get (when $c \rightarrow 0$):

$$\Pi/c = RT/M_n + zRT/M_n \quad (3.4)$$

where RT/M_n is the contribution from the polymer molecule and zRT/M_n from the counterions. Obviously, unless z is accurately known, the molecular weight cannot be determined, and osmotic pressure measurements are not suited for determination of molecular weights of polyelectrolytes in salt-free aqueous solutions. Even very low and sometimes unexpected and unknown amounts of charges on polymers may obscure completely molecular weight determination if performed without salt. An example is given in Fig. 5 [24], where the osmotic pressure of a (1-3)(1-4)- β -D-glucan from oat is given as a function of concentration. This polysaccharide was believed to be a neutral polymer, and the osmotic pressure measurements were first performed in distilled water. As can be seen from the upper curve in Fig. 5, the reduced osmotic pressure (Π/c) increases as the polymer concentration decreases. However, the method may be

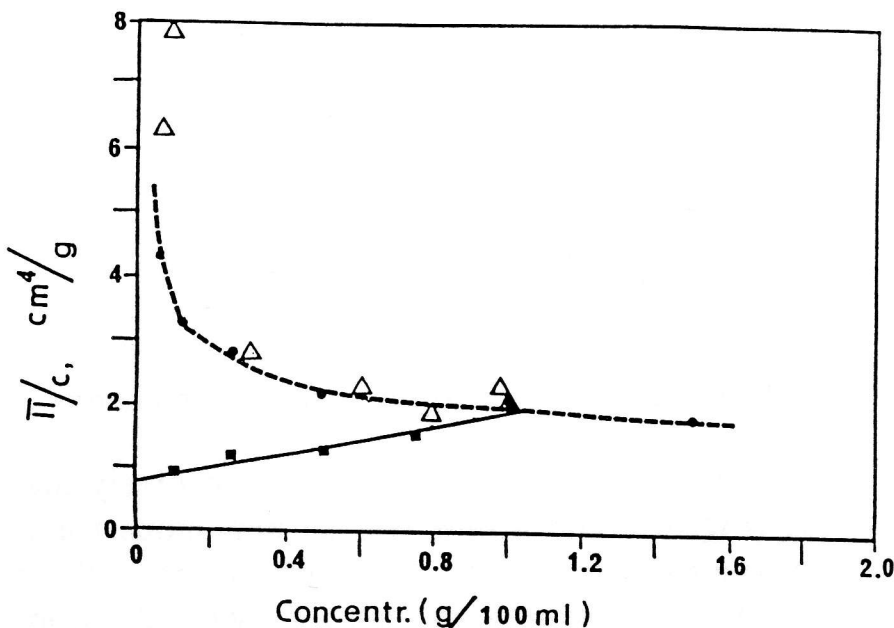


Figure 5. Osmotic pressure determinations of (1-3)(1-4)- β -D-glucan in distilled water (Δ) and in 1M aqueous LiI (\blacksquare). Calculated values in H_2O (\bullet). (From Ref. [24], with permission.)

used to determine the degree of dissociation of counterions:

$$\Pi/c = \Phi(1 + z)RT/M_n \quad (3.5)$$

where Φ is the osmotic activity coefficient related to the fraction of counterions which are dissociated from the polymer molecule. Values of Φ have been determined to be well below 1 for a number of polyelectrolytes [33, 34], which means that the degree of dissociation of counterions from the polymer molecule is well below 100%. This is due to the well-known counterion condensation effect occurring above a critical value of the electrostatic charge density of the polyelectrolyte [35, 36].

With salt (Donnan equilibrium). We will now treat the equilibrium in the osmometer with the presence of a freely equilibrating, ionizable salt B^+X^- in addition to the polyelectrolyte. It was F. S. Donnan in 1911 who pointed out the effect of charged macromolecules (limited to one side of the membrane) on the distribution of small ions across the membrane. We will give here only the results of the distribution of the ions between the two sides of the membrane (Fig. 6 [37]).

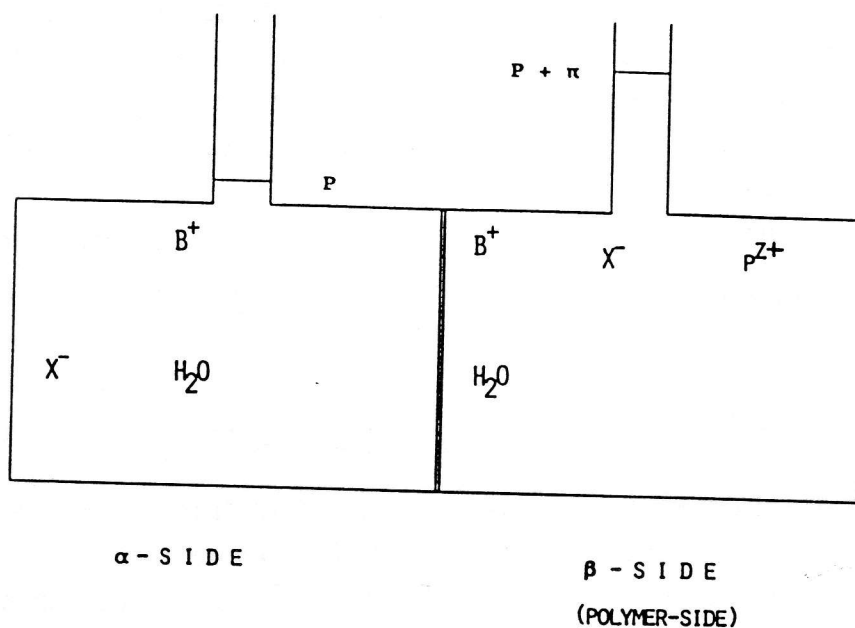


Figure 6. Schematic illustration of the Donnan effect.

We will again consider a polycation. The result from the difference in concentration for *co*-ions (in this example B^+) between the α and β side is:

$$C_B(\alpha) - C_B(\beta) = \frac{-zC_p(\alpha)C_B(\alpha)}{C_B(\alpha) + C_B(\beta)} \quad (3.6)$$

where $C_p(\alpha)$ is the *molar* polymer concentration on the α side, $C_B(\alpha)$ the *molar* concentration of B on the α side and so on. In Eq. (3.6) it is assumed that all the counterions on the polyelectrolyte have dissociated, yielding a contribution $zC_p(\alpha)$ to the concentration of counterions. As discussed earlier, only a fraction (Φ) of the counterions may be dissociated, and reduce the contribution from the counterions to Φz . In any case, this expression will always be negative, so the conclusion is that the *co*-ions are partially *excluded* from the polymer side. The analogous expression for counterions is:

$$C_X(\alpha) - C_X(\beta) = \frac{zC_p(\alpha)C_X(\alpha)}{C_X(\alpha) + C_X(\beta)} \quad (3.7)$$

which shows that the counter-ions are *concentrated* on the polymer side. The conclusion is analogous when dealing with polyanions. *Co*-ions, which are now X^- , are partially excluded from the polymer side, and the counterions, which are now B^+ , will be concentrated on the polymer side.

The Donnan effect will also contribute to the second virial coefficient, which we will now discuss in some detail. In the presence of a salt, it can be shown that the osmotic pressure is proportional to the sum of the differences of the *molar* concentrations of all particles present at equilibrium [14]:

$$\Pi = RT\{C_p(\alpha) + [C_B(\alpha) - C_B(\beta)] + [C_X(\alpha) - C_X(\beta)]\} \quad (3.8)$$

where the symbols are as in (3.6). Combining (3.6), (3.7) and (3.8) gives:

$$\Pi = RT\left\{C_p(\alpha) + \frac{z^2[C_p(\alpha)]^2}{C_B(\alpha) + C_B(\beta) + C_X(\alpha) + C_X(\beta)}\right\} \quad (3.9)$$

In most practical situations, the salt concentration is much larger than the polymer concentration, which implies that $C_B(\alpha) = C_B(\beta) = C_X(\alpha) = C_X(\beta) = C_{BX}$. In the limit, Eq. (3.9) simplifies to:

$$\Pi = RT\left\{C_p(\alpha) + \frac{z^2[C_p(\alpha)]^2}{4C_{BX}}\right\} \quad (3.10)$$

Substituting the weight concentration (c) instead of the molar concentrations (C), we get:

$$\Pi = RT\left\{c/M_n + \frac{z^2c^2}{4M_n^2C_{BX}}\right\} \quad (3.11)$$

By comparing Eq. (3.11) with Eq. (3.2), the second virial coefficient can be identified as $z^2/4M_n^2C_{BX}$, which is called the ideal Donnan contribution. The *observed* second virial coefficient is:

$$B_{\text{obs}} = B_{\text{Donnan}} + B_{\text{neutral}} \quad (3.12)$$

where B_{neutral} is the contribution from the excluded volume effect for a neutral polysaccharide, as discussed in Section 2.

When determining osmotic pressures on polyelectrolytes experimentally, an ionic strength of 0.1 is sufficient to suppress the effect of the charge on the apparent molecular weight, but the Donnan contribution to the second virial coefficient will generally dominate over the excluded volume effect at this salt concentration.

Returning now to Fig. 5, the lower curve shows the normal behaviour of the reduced osmotic pressure as a function of polymer concentration. The solvent here was 1 M LiI.

Another example of the precautions that need to be taken when determining molecular weights of polysaccharides by osmometry has been demonstrated by Fishman *et al.* [38]. They determined the molecular weights of a series of pectins with varying degrees of

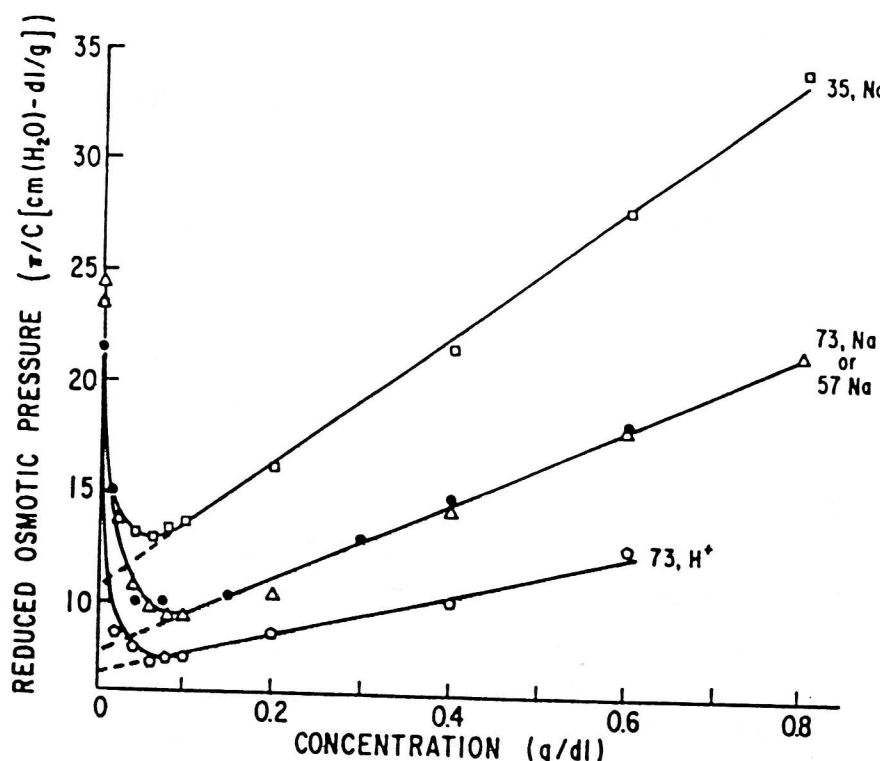


Figure 7. Osmotic pressure measurements on pectins. (From Ref. [38], with permission.)

esterification. Figure 7 shows the results of their osmotic pressure measurements. It can be seen that the reduced osmotic pressure (Π/c) starts to rise when the polymer concentration goes beyond 0.1 g/dl, while the results are as expected for non-associating polymers for the five concentrations from 0.1 to 0.8 g/dl.

The authors explain the behaviour of the pectins by a concentration dependent disaggregation. These authors have used high

Table 4. M_n of some polysaccharide preparations from membrane osmometry.

Polysaccharide	Fraction	Solvent	$10^{-4} \times M_n$	Ref.
Pullulan	P2F3	distilled water	83.4	42
	P16SD5		13.5	
(1-3)(1-4)- β -D-glucan	3 min	1 M LiI	33	24
	25 min		6.3	
Xanthan	XS2H	0.1 M NaCl	12.2	40
	XF3C		23.0	
κ -Carrageenan	1	0.15 M $N(CH_3)_4Cl$	3.2	39
	2		15	
Hyaluronic acid	4	0.5 M NaCl	55	41
	15		268	

performance size exclusion chromatography (HPSEC) and end group titrations to determine M_n of their samples, and their work clearly demonstrates the usefulness of applying different methods for determining molecular weights.

Some examples from the literature of M_n determinations by osmometry are given in Table 4 [39–42], but this is by no means intended to represent a complete survey.

4. STATIC LIGHT SCATTERING

This method is also known as ‘classical light scattering’ and ‘total intensity light scattering’, but we prefer static light scattering as it offers a clear distinction from the different technique of dynamic light scattering (section 6.3). When a solution of macromolecules is illuminated with a beam of light at wavelength λ , the polymer chains will scatter light in direct proportion to their weight-average molecular mass (M_w) and, moreover, the angular dependence of the scattered light at low angles can be related directly to the z-average of the ‘radius of gyration’ (R_G). This is the only technique that can be used to measure the dimensions of the molecules *without any assumptions about the shape of the molecule*. Light scattering is also an *absolute* method for determining these molecular parameters, as opposed to viscometry and gel permeation chromatography which requires calibration. The method is the major technique for determining M_w of polysaccharides. The main experimental difficulty of the method is the demand for high quality solutions free of dust and aggregates.

4.1 General Background

4.1.1 Light Scattering from Solutions of Small Macromolecules ($R_G < \lambda/20$)

In 1871 Lord Rayleigh published [43] the theory of the scattering of light by free and independent moving gaseous particles much smaller than the wavelength of light. We will only give the equations for the *excess* scattering of the polymer molecules, where the solvent scattering is subtracted out. For a more detailed treatment of the theory, the reader is referred to Tanford [14] or Kratochvil [44].

For a small particle ($R_G < \lambda/20$) in the limit of infinite dilution, it can be shown that the ratio of the intensities between unpolarized incident light (I) and scattered light (I_s) is:

$$\frac{I}{I_s} = \frac{2\pi^2 n_0^2 (\text{dn/dc})^2 (1 + \cos^2 \theta)}{N_A \lambda^4 r^2} c M_w \quad (4.1)$$

where n_0 is the refractive index of the solvent, dn/dc is the specific refractive increment of the solute-solvent system, θ is the angle of observation, N_A is the Avogadro number, M_w is the weight-average molecular weight of the solute, λ is the wavelength of incident light and r is the distance between the sample and the detector. If vertically polarized light is used the $(1 + \cos^2 \theta)$ term is not required. The specific refractive increment (dn/dc) is a characteristic of a polymer-solvent system at a given temperature, and can be experimentally determined in a differential refractometer, or in many cases it can be found in the literature [45]. Equation (4.1) can be rearranged:

$$(I/I_s) \cdot \frac{r^2}{(1 + \cos^2 \theta)} = \left[\frac{2\pi^2 n_0^2 (\text{dn/dc})^2}{N_A \lambda^4} \right] c M_w \quad (4.2)$$

The term in brackets on the right-hand side turns out to be a constant (K) for a particular solute-solvent system, and the left-hand side is called the Rayleigh ratio (R_θ), which can be evaluated in absolute terms, simplifying Eq. (4.2) to

$$R_\theta = K c M_w$$

or

$$K c / R_\theta = 1 / M_w \quad (4.3)$$

which is valid for an ideal solution.

At this point it is necessary to say something about the scattering of light in a crystal, in an ideal gas and in a pure liquid. A perfect, infinitely large, crystal does not scatter light at all, but real crystals scatter light due to the occurrence of crystal lattice defects. The intensity of light scattered by a unit volume of an ideal gas (highly diluted) is directly proportional to the number of molecules in this volume. Pure liquids scatter light substantially less than the same number of molecules in the gaseous state but more than a real crystal. The reason for this is that in a real solution it will be fluctuations in the number of particles in a volume element which give rise to fluctuations in the density of the liquid and therefore also the refractive index.

Returning to a *solution*, where we will again only consider the excess scattering from the solute molecules, it can be shown that the intensity of the scattered light is related to the increase of the osmotic pressure with concentration ($d\Pi/dc$) [46]:

$$R_\theta = (KcRT)/(d\Pi/dc) \quad (4.4)$$

Insertion of the derivative of Eq. (3.1) yields:

$$Kc/R_\theta = 1/M_w + 2Bc + 3Cc^2 + \dots \quad (4.5)$$

where B is the second virial coefficient and C the third virial coefficient. By analogy with osmometry, we need only to consider the second virial coefficient for dilute solutions, simplifying Eq. (4.5) to

$$Kc/R_\theta = 1/M_w + 2Bc \quad (4.6)$$

This equation is used for determining the molecular weight and the second virial coefficient for polysaccharides where R_G is smaller than $\lambda/20$. If, for example, $\lambda = 500$ nm it means R_G has to be less than 25 nm.

4.1.2 Light Scattering from Solutions of Large Macromolecules ($\lambda/20 < R_G < \lambda/2$)

The equations considered so far are only valid for polysaccharides with R_G less than $\lambda/20$. For larger molecules there will be more than one point in each molecule that will scatter light, making the angular dependence more complex. The effect can be visualized when observing a beam of sunshine in a dusty room. The dust particles are much easier to see when the observer is looking *against* the sun compared to looking *away* from it. The reason is that the large dust particles scatter more light forward (small angles) than backward (large angles). A cross-section of a ‘scattering envelope’ produced when unpolarized incident light is scattered from small and large molecules is given in Fig. 8.

The intensity of the scattered light as a function of the scattering angle [which is called the particle scattering function $P(\theta)$] for different types of molecules will not be considered here, but can be found elsewhere [14, 44].

An important conclusion from these calculations is that at low scattering angles and low polymer concentrations, the dimensions of the molecules can be calculated as a z-average of the radius of gyration, without any assumptions about the shape of

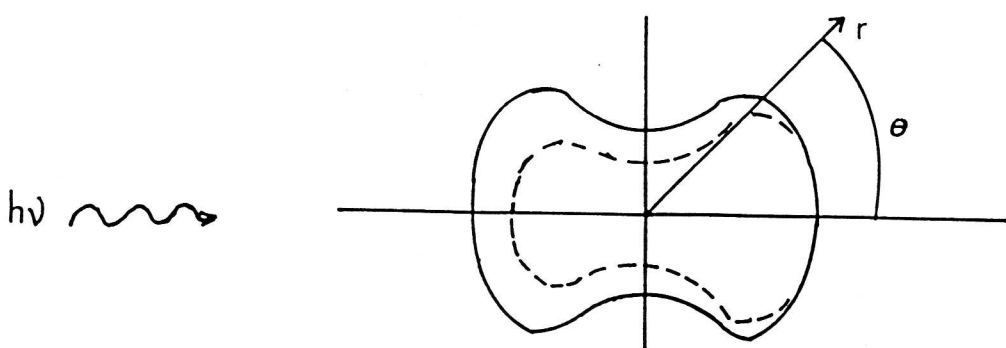


Figure 8. Angular dependence of the intensity of scattered light by a particle. Incident light unpolarized. Solid line: scattering profile for 'Rayleigh scattering' (small particle). Broken line: Rayleigh-Gans-Debye scattering (larger particle). (From Ref. [14], with permission.)

the macromolecule (compact sphere, coil, stiff rod). For larger molecules, Eq. (4.6) can be modified to (dilute solutions):

$$Kc/R_\theta = [1/P(\theta)](1/M_w + 2Bc) \quad (4.7)$$

The particle scattering function $[P(\theta)]$ can be shown to be:

$$1/P(\theta) = 1 + (16\pi^2 R_G^2/3\lambda^2) \sin^2(\theta/2) \quad (4.8)$$

for small angles.

Combining Eq. (4.7) with (4.8) we get

$$Kc/R_\theta = [1 + (16\pi^2 R_G^2/3\lambda^2) \sin^2(\theta/2)](1/M_w + 2Bc) \quad (4.9)$$

The validity of Eqs. (4.7)–(4.9) depends on there being no significant changes of phase or other distortions of the incident electric vector induced by the particle. This is known as the 'Rayleigh-Gans-Debye' criterion (see, e.g. ref. 44), and is generally satisfied for polysaccharides of $M \lesssim 20 \times 10^6$.

Now, since Eq. (4.9) is only valid at high dilution and low scattering angles, it is necessary to extrapolate data at each angle to zero concentration before the radius of gyration can be calculated, and to extrapolate the data at each concentration to zero angle to calculate the molecular weight and the second virial coefficient. This is most conveniently done in a Zimm plot where Kc/R_θ is plotted against $\sin^2(\theta/2) + kc$, where k is an arbitrary constant (positive or negative) which is used to spread the data on the graph. Therefore, in a light scattering experiment the scattering from a number of concentrations of polysaccharide is measured at different angles. Figure 9 shows a schematic drawing of a light scattering photometer.

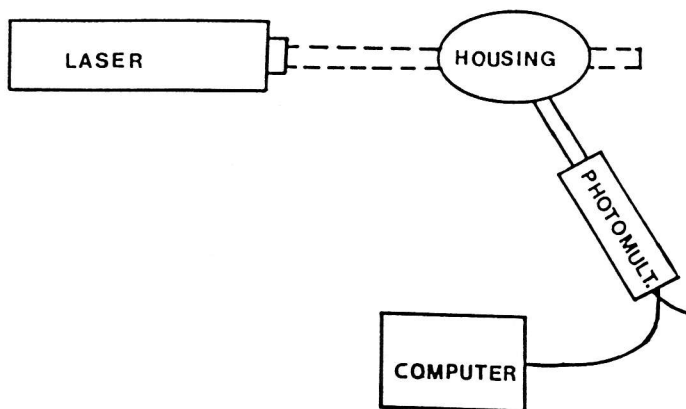


Figure 9. Schematic diagram of apparatus for (static) light scattering measurements.

Equation (4.9) is the basis for the conventional way of presenting light scattering data, the Zimm plot [47], which uses biaxial extrapolation. An example (Dextran T-500) is shown in Fig. 10. Points with constant c ($= c_y$) are extrapolated to $\theta = 0$, which is the abscissa value where $\sin^2(\theta/2) = 0$, i.e. $k c_y$. Points with constant θ ($= \theta_x$) are extrapolated to $c = 0$, which is the abscissa value $\sin^2(\theta_x/2)$. The lines

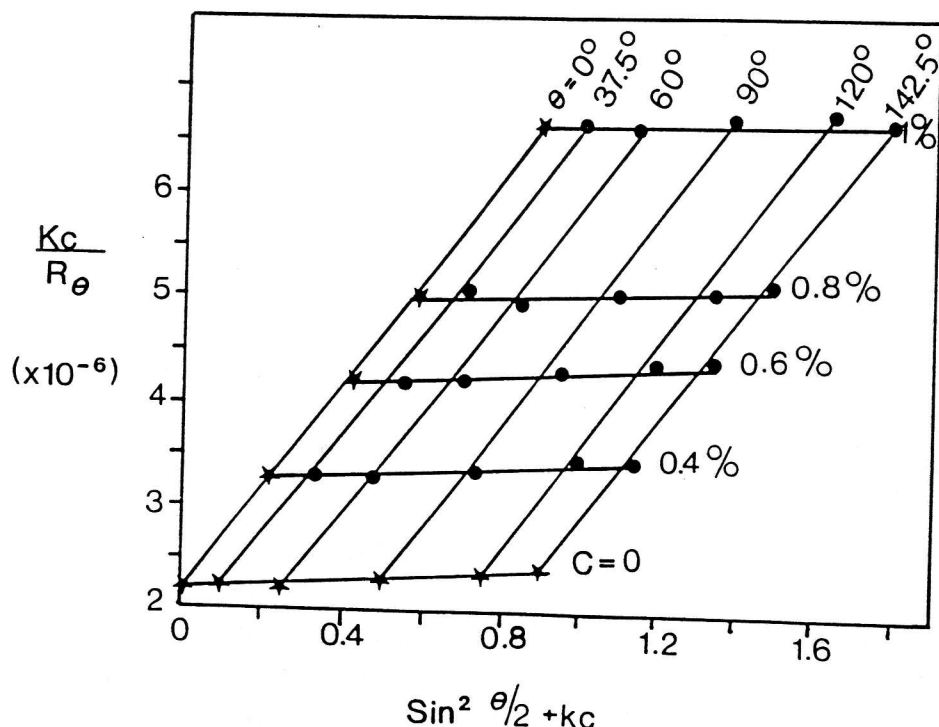


Figure 10. Zimm plot for extrapolation of light scattering data. The sample is dextran T-500 in distilled water. (K.M. Vårum, unpublished observations.)

for zero concentration and zero angle are then extrapolated to the same ordinate value, which equals $1/M_w$. The slope of the zero concentration line equals $(1/M_w)(16\pi^2 R_G^2/3\lambda^2)$, and the slope of the zero angle line equals $2B/k$, thus providing estimates of the radius of gyration and the second virial coefficient.

As mentioned above, optically clear solutions are required for light scattering experiments. An example of the extreme caution needed in interpreting light scattering data is provided by Smidsrød and Haug [48]. They investigated filtered alginate solutions and obtained reasonable values for both the molecular weight and the radius of gyration. However, the small negative value obtained for the second virial coefficient made the authors suspicious, as alginate is a highly charged polyelectrolyte. Centrifugation of the solutions showed that the second virial coefficient increased markedly with the time of centrifugation. The authors were also able to isolate the impurity that had caused the anomalies. The work clearly demonstrates the importance of the clarification procedure and the need for skilled experimentalists.

4.2 Polyelectrolytes

In general, the light scattering theory is valid for polyelectrolytes if neutral salts are added to the system as in osmometry. However, some precautions specific to the light scattering system should be taken. When determining dn/dc (the specific refractive increment) for a polyelectrolyte this should be done in the same salt system as used in the light scattering experiments. Moreover, measurements of the difference in refractive index of the polyelectrolyte and the solvent should be carried out at constant chemical potential of both the polyelectrolyte and the salt molecules. This means that the polyelectrolyte solutions must be extensively dialysed against the solvent containing the salt molecules prior to refractive index measurements [49, 50]. As in osmometry, molecular weights cannot be determined at very low salt concentrations, but for a completely different reason. At very low salt concentrations (below $I = 0.01$) polyelectrolytes may show liquid crystal behaviour or correlated molecular movements even at extremely low polyelectrolyte concentration [51]. This will violate the basic assumptions made by Rayleigh about free and independent movement of the particles.

4.3 Clarification of Solutions

Light scattering methods were described by Flory [52] to be painstaking and the work needed for obtaining clean solutions cannot be overestimated. Even traces of dust and/or aggregates may lead to incorrect estimates of the molecular weight, as light scattering yields the *weight average* M_w . A more detailed procedure for clarification and preparation of polymer solutions is given by Tabor [53]. We will here propose a rather simple and general procedure for preparation of polysaccharide solutions.

4.3.1 Ultrafiltration

A large variety of membrane filters with well-defined pore-sizes are commercially available. We recommend the following sequence of pore sizes to be used in series: 1.4, 0.8, 0.4 and 0.2 μm . Depending on the size of the polysaccharide under investigation, the upper or lower pore size may be excluded. Disposable filters are practical, but also more expensive.

It is also important that the light scattering *cells* are free of dust. This may conveniently be done by flushing the cells with air filtered through a 0.2 μm filter. The dust free cells are then covered with Parafilm, and the polysaccharide solution may then be filtered directly into the cell through the Parafilm by the use of a needle. The solution in the light scattering cell is then covered with another layer of Parafilm.

4.3.2 Ultracentrifugation

It is necessary to use high speed centrifugation if the solutions after ultrafiltration contain aggregates. Caution must be taken to ensure that the individual polysaccharide molecules do not sediment together with aggregates and dust, as this technique is also used for sedimentation analysis of polysaccharides (Section 5). Dependent on the particular polymer-solvent system under investigation, centrifugation times between 30 min and 4–5 h are needed and a centrifugal force of at least 30 000 g should be used. For the removal of all aggregates, up to 300 000 g may be necessary.

The best option is if the solutions can be ultracentrifuged directly in the light scattering cells. If mechanical shocks are avoided, the dust and aggregates can be retained at the bottom of the cell during

Table 5. Examples of M_w values for polysaccharide preparations using static light scattering.

Polymer	Solvent salt type	I^a (M)	(dn/dc)		$10^{-3} \times M_w$ (g/mol)	Fraction	Ref.
			ml/g	λ (nm)			
Alginate	Aq. NaCl NaF Aq. NaCl	0.09 0.01 0.5	0.165 0.140	436 436	525 69 320	fraction 4 fraction 15 fraction 21	48 41 54
Hyaluronic acid					1030	H_{20}	HMR
κ -Carrageenan	Aq. NaCl EDTA $T = 20^\circ C$	0.2 0.005	0.118 ± 0.003	546	44 522	P100	55
	Aq. KCl Na-acetate Milli-Q water	0.4 0.05	0.165 ± 0.001	488	718 145 ± 5		
Meningococcal polysaccharide					< 100		
Pullulan					2080 ± 208	P1F1 P2F3	42
Schizophylan	NaOH	0.01 N	0.144 0.142	436 546	992 ± 99 196 ± 20	PN6SD5 $H-5$	56
Xanthan	Aq. NaCl	0.1	0.144 ± 0.002	436	259 620	K-4 $S-65-2$	40
	Aq. NaCl	0.1		647.1	4000 140 ± 10 680 ± 120 1500 ± 170 2940 1370	XF5C XF3 XF1 NX PFX	57

^a I = ionic strength (mol/l); M = molarity (mol/l).

the time it takes to collect the light scattering data. Alternatively, if the necessary precautions are taken, the solutions may be transferred from the centrifuge cell to the light scattering cell, but it is then recommended that this is done in a dust-free environment, e.g. a sterile bench where the air is filtered through a $0.2\text{ }\mu\text{m}$ filter.

4.4 Recent Developments and Applications

Most modern light scattering experiments are performed using a laser as the light source. Indeed it is fair to say that the advent of the laser has provided a major stimulus to the light scattering technique over the last 10–15 years. The properties of high intensity, collimation and monochromaticity were immediately recognized as advantageous in improving the quality of the angular intensity envelope. The additional property of coherence gave rise to the new technique of dynamic light scattering, and the consequences of this in the context of polysaccharide molecular weights is discussed in Section 6.3. Commercial instruments, although principally designed for dynamic light scattering, can also be used as a static device provided that the appropriate calibration checks and realignments are made.

Examples from the literature of polysaccharide molecular weights determined by SLS are numerous. Table 5 [54–57] gives only a selection and contains values from various instruments. Where serious disagreement with other techniques (yielding M_w) occurs, it is normally associated with problems of clarification of solutions with the former technique (see, e.g. Smidsrød and Haug [48]). Our view is that light scattering should not, where possible, be used in isolation but in conjugation with other techniques.

5. SEDIMENTATION EQUILIBRIUM

If polysaccharides are the ‘Cinderella molecules’ of Biochemistry (F. Franks, personal communication) then sedimentation equilibrium is the Cinderella technique. It is fair to say that there is less than a handful of operators actively engaged in applying the technique to polysaccharide analysis. Indeed the same is true for all other classes of macromolecule, both naturally occurring and

synthetic, and indeed for other types of analytical ultracentrifuge measurement such as sedimentation velocity or zonal diffusion. At the time of writing, analytical ultracentrifuges, such as the Beckman Model E, the MSE Mk. II or the MSE Centriscan are no longer commercially available, although scanning Schlieren or absorption optics attachments have been available for some preparative machines (such as the Beckman LX80). The methodology however continues to be developed (particularly for low speed sedimentation equilibrium) as a powerful tool for the characterization of difficult heterogeneous polymer systems—the hallmark of polysaccharides—whose molecular weights cannot be obtained by simple electrophoretic techniques or simple calibration of gel permeation chromatography columns. Significantly, a new generation of analytical ultracentrifuge is being planned [58].

5.1 Some Basic Theory

There are many books [59–63] and reviews [64–67] on the sedimentation equilibrium technique. One particularly useful source is that of Creeth and Pain [66] from which the following summary of basic theory is given. For a solute at sedimentation equilibrium there is no net transport of solute: the distribution of solute is solely a function of the thermodynamic (rather than hydrodynamic) properties of the system. For polysaccharides such an equilibrium distribution is generally achieved in 24–48 h depending on the nature of the solute and the experimental conditions (rotor speed, temperature, etc.). The most accurate method of recording solute distributions at sedimentation equilibrium is the Rayleigh Interference optical system which gives a direct record of solute concentration relative to the meniscus as a function of radial displacement from the centre of the rotor. Using an appropriate data capture facility Rayleigh patterns such as shown in Fig. 11 can be transformed into plots of $\log_e J$ versus r^2 , where J is the absolute concentration (expressed in fringe displacement units) and r is the distance of a given point in the cell from the centre of the rotor (see, e.g. Fig. 12). From these plots the various molecular weight averages (usually the weight average) can in principle at least be extracted. Other (less precise) optical systems are available (see Schachman [59] and Lloyd [68] for a discussion on these). The absorption optical system, popular in

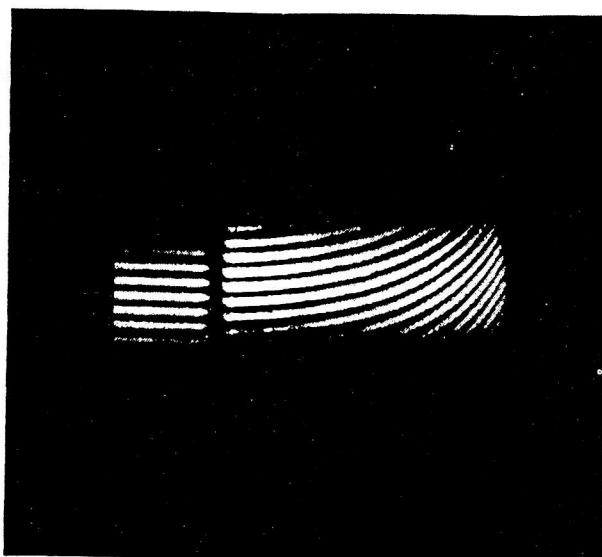


Figure 11. Rayleigh interference fringes for pectins (from ripe tomato cell walls) at sedimentation equilibrium. Mercury arc light source. Rotor speed = 9341 rev/min. Temperature = 20.0°C. Loading concentration ~ 0.4 mg/ml. Solvent pH = 7.0; $I = 0.10$. Air fringes (part thereof) to the left; solution fringes to the right.

protein and DNA biochemistry, principally because of the smaller amounts of sample required, is not generally usable for most polysaccharides (because of the lack of an appropriate chromophore). The Schlieren optical system, most popular with sedimentation velocity (see below), can be used to record solute distributions at sedimentation equilibrium. The record is one of the refractive index gradient versus radial displacement and can be most readily transformed into 'Lamm plots', i.e. $\ln [1/r(dJ/dr)]$ versus r^2 , and yields the z-average molecular weight as the primary parameter. Its principal disadvantages are that solute distributions cannot be recorded as accurately as with Rayleigh optics and that higher solute concentrations are generally required.

The fundamental equation representing distribution of solute at sedimentation equilibrium can be written, for an ideal system as [66]

$$\frac{d \ln J}{d(r^2)} = \frac{M_w(1 - \bar{v}\rho)\omega^2}{2RT} \quad (5.1)$$

where r is the radial displacement, ω is the rotor speed (rad/s), \bar{v} the partial specific volume (ml/g) and ρ the solution density (g/ml).

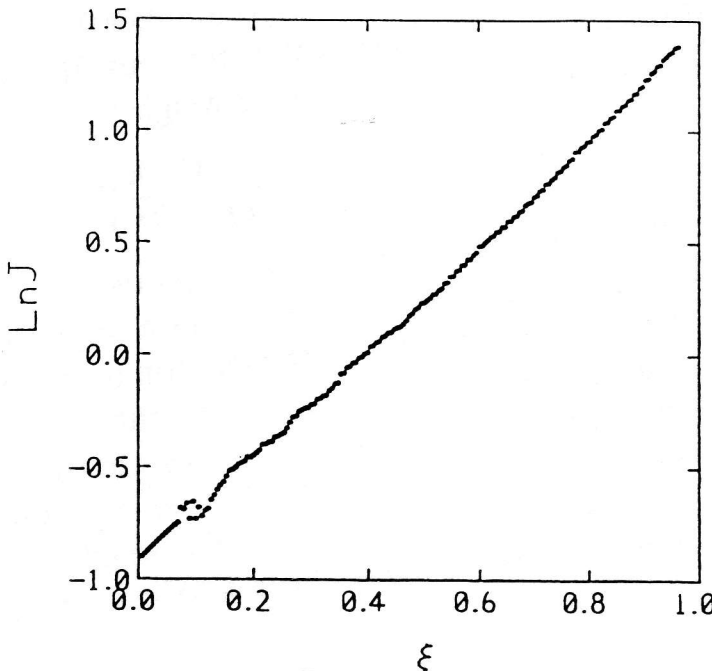


Figure 12. Log fringe concentration J versus radial displacement squared parameter ξ from a low speed sedimentation equilibrium experiment on wheat β -D-glucan. $\xi = (r^2 - a^2)/(b^2 - a^2)$, where r is the radial displacement at a given point in the cell, and a and b the corresponding values at the meniscus and cell base, respectively. Instrument: Beckman Model E equipped with laser light source. Rotor speed = 7440 rev/min. Temperature = 20.0°C. Loading concentration ~ 0.4 mg/ml. Solvent pH = 7.0, $I = 0.10$. Data captured on LKB gel scanner (see text). (K. M. Vårum, S. E. Harding and O. Smidsrød, unpublished observations.)

This represents the distribution of solute at equal total potential throughout the centrifuge cell. From a simple rearrangement of this equation the point (weight) average molecular weight can be defined:

$$M_w(r) = \frac{d \ln J}{d(r^2)} \frac{2RT}{(1 - \bar{v}\rho)\omega^2} \quad (5.2)$$

$M_w(r)$ as a function of r^2 can thus readily be obtained from, for example, sliding strip quadratic fitting procedures to the $\ln J$ versus r^2 data. It is also possible to obtain—provided the data is good enough—the point *number*-average molecular weights (see, e.g. Teller [67]):

$$M_n(r) = \left[\frac{J}{\int_a^r J d(r^2) + \{J(a)[2RT/(1 - \bar{v}\rho)\omega^2] \cdot 1/M_n(a)\}} \right] \frac{2RT}{(1 - \bar{v}\rho)\omega^2} \quad (5.3)$$

where $J(a)$ is the concentration (fringe numbers) at the meniscus and $M_n(a)$ is the number average at the meniscus. It is also possible to obtain the z-point-average molecular weight:

$$M_z(r) = M_w(r) + \frac{2RT}{\omega^2(1 - \bar{v}\rho)} \frac{d \ln M_w(r)}{d(r^2)} \quad (5.4)$$

To obtain reliable values for $M_n(r)$ or $M_z(r)$ requires data of the highest possible precision or very heavy data smoothing: point number averages involve a difficult extrapolation to the meniscus to obtain $M_n(a)$; z-averages require essentially a double differentiation of the basic fringe data unless Schlieren optics are used to yield a Lamm plot which gives z-averages directly (see, e.g. Bowen [69]).

The second basic way of obtaining molecular weight information is to define an average slope for the whole distribution (e.g. Creeth and Pain [66]):

$$M_w^0 = \frac{J(b) - J(a)}{J^0(b^2 - a^2)} \frac{2RT}{\omega^2(1 - \bar{v}\rho)} \quad (5.5)$$

(whole-cell weight average)

$$M_n^0 = \frac{J^0(b^2 - a^2)}{2 \int_a^b [J(r)/M_n(r)]r dr} \quad (5.6)$$

(whole-cell number average)

$$M_z^0 = [M_w(b)J(b) - M_w(a)J(a)]/[J(b) - J(a)] \quad (5.7)$$

(whole-cell z-average)

where a and b are the radial displacements at the cell meniscus and base respectively, and J^0 the initial loading concentration (in fringe numbers).

The most extractable whole cell average from this technique is the weight average (Eq. 5.5), but its extraction can involve a difficult extrapolation of the fringe data to the cell base. The use of a recently described operational point average (M^*) appears to be of some value here. The M^* function, defined by [70]

$$M^*(r) = \left\{ j(r) / \left[J(a)(r^2 - a^2) + 2 \int_a^r r j dr \right] \right\} \{2RT/[\omega^2(1 - v\rho)]\} \quad (5.8)$$

[where $j(r)$ is the (fringe) concentration relative to that at the meniscus] has several properties which may be advantageous for the handling of polysaccharide data—one of these is that its value extrapolated

Table 6. Comparison of M_w^0 values obtained via ($\ln J$ or M^*) extrapolations [70].

	I	II	III	IV	V
$\ln J$	6.59×10^5	4.73×10^6	2.45×10^6	2.15×10^6	4.99×10^5
M^*	6.64×10^5	4.87×10^6	2.77×10^6	2.63×10^6	5.00×10^5
Theoretical	6.67×10^5	4.84×10^6	3.02×10^6	3.02×10^6	5.00×10^5
System I	Two component mixture, $M_2 = 3M_1$; $c_2^0 = 0.167 c_1^0$ ($M_1 = 5 \times 10^5$)				
System II	Very polydisperse (log-normal: $\sigma/\log M_w = 0.044$; $M = 1-15 \times 10^6$)				
System III	Isodesmic assn. $c = 1$, $k = 2$ ($M_1 = 5 \times 10^5$)				
System IV	As III but with fringe data with $\pm 2 \mu$ standard error				
System V	Single solute, $M = 5 \times 10^5$, fringe data with $\pm 2 \mu$ standard error				

to the cell base equals the M_w over the whole solute distribution [70]. This generally offers a more convenient extrapolation procedure for the extraction of M_w^0 data (Table 6 [70]).

It is also possible in theory to get whole cell number and z-averages (Eqs 5.6 and 5.7) but, as with point averages, this requires data of the highest precision. As before, the Schlieren optical record yields directly the z-average molecular weight as opposed to weight average from conventional Rayleigh records.

5.2 Low Speed Versus High Speed Sedimentation Equilibrium

One of the major inconveniences of the sedimentation equilibrium method (using Rayleigh optics) is that the optical records are of fringe displacement or concentration relative to that at the meniscus, as opposed to absolute fringe displacement values. Denoting j as the relative (fringe) concentration, then the absolute (fringe) concentration J is defined by [66]

$$J = J(a) + j \quad (5.9)$$

where $J(a)$ is the meniscus concentration. To obtain molecular weight information from the basic fringe data $J(a)$ has to be obtained. Creeth and Pain [66] have considered in detail the many procedures (overspeeding, synthetic boundary measurements, conservation of mass calculations, etc.) available for the extraction of

$J(a)$. A very popular alternative in the protein biochemistry field has been to employ the high speed or meniscus depletion method of Yphantis [71] based on an earlier proposal by Wales *et al.* [72]. This yields an effective $J(a)$ of 0 and also permits the direct extraction of $M_n(r)$ and M_n^0 values without the need for $M_n(a)$. Yphantis, in his original paper [71], gave the many conditions for the applicability of the method, conditions which are unfortunately sometimes ignored in the literature. The same conditions have been further stressed by Fujita [63]. The chief disadvantage with the high speed method is that the fringe displacements are compressed into a relatively short region of the cell making data capture difficult. It should also be stressed that for polydisperse systems like polysaccharides the method is not generally applicable because of the normal impossibility of getting proper depletion at the meniscus without losing optical registration of the fringes at the cell base. The high speed method also magnifies the effective non-ideality of the system because of a speed dependence effect (see, e.g. Fujita [63], Creeth and Knight [73] and Eq. 5.11 below). A common pitfall is to assume depletion conditions when clearly this is not valid—the temptation being the analyses are a lot easier to perform. There are, however, now available routine procedures for obtaining menisci concentrations by appropriate mathematical manipulation of the fringe data. For example, $J(a)$ can be obtained from twice the ratio of the intercept of a graph of $j/(r^2 - a^2)$ versus $(\int_a^r rjdr)/(r^2 - a^2)$ to the limiting slope [70]. Teller *et al.* [74] list other manipulations which similarly yield $J(a)$. Simulations of model polydisperse systems have shown that over the upper third of the solution column at an appropriate speed a linear extrapolation gives $J(a)$ to better than 15%. As speeds are such that $J(a)$ is approximately 0.5 or less this is quite adequate for most purposes. For very polydisperse systems a linear extrapolation becomes less appropriate: the value of automatic data capture and multiple data acquisition/statistical smoothing for polysaccharides is therefore clearly indicated.

5.3. Sedimentation Equilibrium and Thermodynamic Non-ideality

In Section 2.2. we discussed the non-ideality of polysaccharides in relation to molecular weight determination. For the case of sedimentation equilibrium, all the molecular weight averages

referred to in Section 5.1 above are apparent values, i.e. influenced by thermodynamic non-ideality: the relation between apparent and ideal weight averages can be written, correct to first order in the virial expansion as [75, 76]:

$$1/M_{w,app} = (1/M_w)[1 + (2BM - \bar{v})c + \dots] \quad (5.10)$$

where B is the colligative second virial coefficient. Similar expressions are available for the number and z-averages. The \bar{v} term is missing in Tanford [15], Tombs and Peacocke [21] and Fujita [63] but is present in Ross and Minton [75] and Harding and Johnson [76] (although it is not generally significant for most macromolecular systems, apart from compact globular macromolecules). Fortunately, if the solvent density ρ_0 is used in Eqs. (5.1–5.8) instead of the solution density ρ the \bar{v} term to a very good approximation disappears (see Eq. 5.12 of ref. 63).

If the initial cell loading concentrations c^0 are used in Eq. 5.10 (and the M_w , $M_{w,app}$ refer to M_w^0 , $M_{w,app}^0$ values, respectively), the complete equation for departure from ideal behaviour also includes a speed dependence term, which may be significant at high speeds or for relatively large solution column lengths [63]:

$$B_{eff} \approx B(1 + \lambda^2 M_z^2/12) \quad (5.11)$$

where B_{eff} is the effective virial coefficient and λ a term defined by

$$\lambda = (1 - \bar{v}\rho_0)\omega^2(b^2 - a^2)/2RT \quad (5.12)$$

This extra term can be minimized by using low rotor speeds and short (3 mm or less) solution column lengths. This has been discussed in some detail by Fujita [63] and Suzuki [77]. However, if the high speed method is attempted this parameter can become significant.

Non-ideality can be tackled in several ways. (a) Firstly by working at very low solute concentrations (0.2–0.4 mg/ml or less) in long path length cells (e.g. Beckman 30 mm, MSE 20 mm). The high speed meniscus depletion method should of course be avoided and small column lengths should be employed (3 mm or less). These precautions are normally sufficient to avoid serious error in the calculated molecular weight parameters. For more extreme cases one of the following further steps can be taken. (b) Extrapolate the point (normally weight) average molecular weight (or the reciprocal thereof) to zero concentration, data taken from a single experiment. Although this counters non-ideality, if there is significant

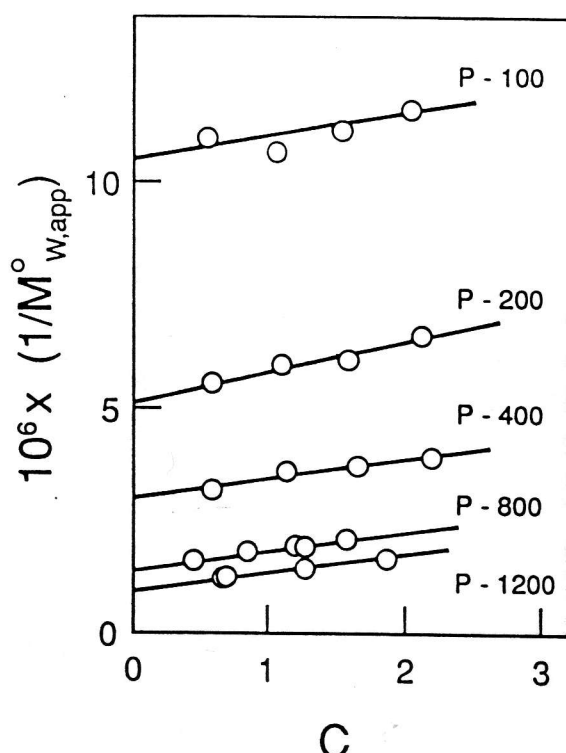


Figure 13. Extrapolation of apparent 'whole-cell' weight average molecular weights to zero concentration for pullulan fractions. $c = (c_a + c_b)/2$, where c_a is the concentration at the cell meniscus and c_b at the cell base. (From Ref. [23], with permission.)

redistribution of the solute components relative to each other, the resulting extrapolated value will be biased towards the low molecular weight end of the distribution. Again this bias can be minimized by use of low speeds and short solution columns. (c) Extrapolate the whole cell weight average to zero concentration (several experiments). This is illustrated by Fig. 13. This is the most rigorous method of dealing with non-ideality but is also the most time consuming. However, the use of multichannel cells (e.g. of the 'Yphantis' type [78]) can be a great time saver. (d) The use of compound point-average molecular weights (such as M_{y1} , M_{y2}) which are free of first-order effects of non-ideality (but also polydispersity). These are defined by Roark and Yphantis [79].

5.4 Polydispersity Versus Self-association Phenomena

It is normally impossible to distinguish in a single sedimentation equilibrium experiment between the effects of polydispersity (i.e. the presence of non-interacting components of different molecular

weight and/or partial specific volume) and self-association phenomena [79]. Although for many cases this may not be important since only a small proportion of polysaccharides are thought to self-associate, for some like guar the ability to distinguish these effects may be significant. There are two possible routes. (a) Use of non-dissociating versus dissociating solvents. Depending on the nature of the suspected interaction appropriate dissociative solvents could be used; e.g. change of ionic strength or pH for suspected charge interactions, inclusion of SDS to suppress hydrophobic interactions or guanidine hydrochloride for hydrogen bond interactions. The latter has the advantage that because of the high molarity required (6 M), and since this reagent is almost totally dissociated the ionic strength is also high ($I = 6.0$). Use of this type of assay is of course not exclusive to sedimentation equilibrium! (b) Use of diagnostic plots. There are several diagnostic plots available to distinguish polydispersity from self-association behaviour (see, e.g. Roark and Yphantis [79]) and all involve a combination of different experimental data sets of point averages taken at different initial loading concentrations. These can be applied even if non-ideality is significant. Although this has had application in the related field of glycoconjugates [80, 81] it has not, as far as we are aware, been applied to systems of polysaccharides: the potential for the analysis of, for example, guar or β -glucans—both of which are thought to self-associate—is, however, clearly indicated.

The effects of either self-association or polydispersity can be suppressed by the effects of non-ideality which tends to produce opposite curvature in plots of $\ln J$ versus r^2 . Linearity of one of these plots is therefore insufficient criterion—taken by itself—for sample homogeneity or thermodynamic ideality [82]. A simple diagnostic check is, however, available involving the use of multi-channel cells and different cell loading concentrations [83].

Assuming polydispersity and/or association behaviour have been diagnosed in a particular system it is possible to obtain more specific parameters to represent such behaviour. For example, there is an extensive literature on the characterization of associating systems by sedimentation equilibrium, a literature which also includes a proper consideration of thermodynamic non-ideality (for a review, see Kim *et al.* [84]). For the case of polydisperse characterization—in terms of molecular weight distribution analysis—several approaches are available. The simplest is to use ratios of

(whole cell) molecular weight averages, e.g. M_z/M_w or M_w/M_n (cf. Section 2.1.). The second way is to model directly plots of $\ln J$ versus r^2 , but this involves the solution of non-linear equations which are linked in a complicated inter-dependent way, and this generally takes a great toll on computer resources [85]: it has not yet been applied to polysaccharides although it has been used to model discrete distributions of molecular weight which at least partially describe mucus glycoproteins [85]. The third and easiest method—and by the far the most successful—is to use sedimentation equilibrium as an off-line calibration procedure for GPC and this is considered in Section 8.1.

5.5 Other Advances in Theory and Methodology

Besides improvements in the methodology for the modelling of molecular weight distributions there have been other advances potentially advantageous for polysaccharide analysis. We note here: (a) The ability to model solute distributions for systems that are both polydisperse and associating [86]. (b) Improvements in the data handling of self-associating systems [87]. (c) Improvement in the resolution of the fringe data: all commercial analytical ultracentrifuges have, to date, been supplied with conventional Hg-arc light sources or similar. In the 1970s several users replaced these with small lasers to enhance the quality of the Rayleigh patterns (see, e.g. Williams [88], Laue and Yphantis [89], Yphantis [90] and Laue *et al.* [91]). For polysaccharides this is important, particularly if more sophisticated analyses involving number, z and 'compound' averages are being sought. (d) Improvement in data capture facilities. One of the reasons for the decline in popularity of sedimentation techniques has been the tediousness of manually measuring up Rayleigh fringes patterns. This has been ably illustrated by a classic quote of Teller in his 1973 review [67]. In the 1970s automatic plate readers appeared [92–94] but were never commercially available. A much more recent development has been the adaptation of a commercially available scanning laser densitometer—primarily intended by the manufacturer (LKB, Bromma) for the capture of gel electrophoresis data—to capture automatically sedimentation equilibrium Rayleigh interference data [95, 96]. Using a simple Fourier series algorithm fringe displacement, $j(r)$ versus radial

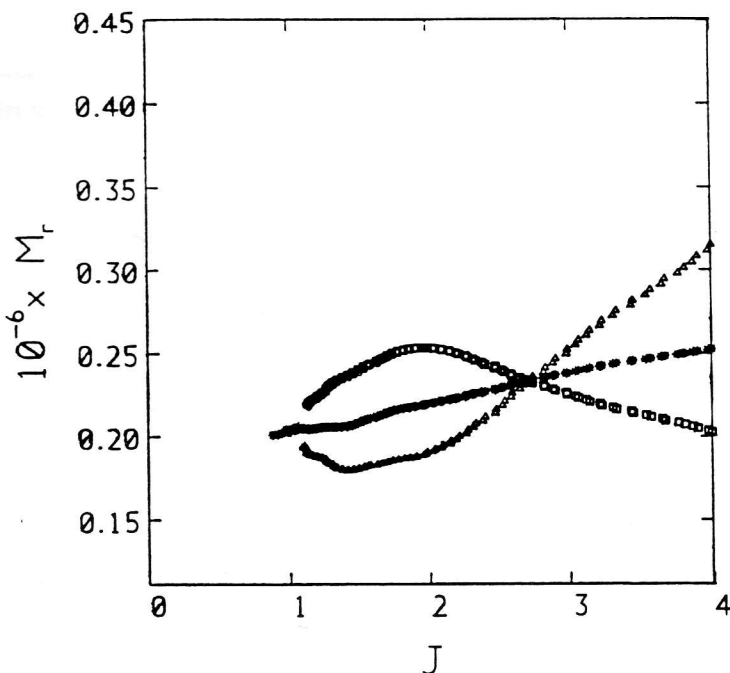


Figure 14. Plot of (apparent) point average molecular weights for wheat β -D-glucan. Run/sample details as Fig. 12. (*) M_w ; (□) M_z ; (Δ) M_{y^2} .

displacement r , data can be accurately obtained, and an example of point molecular weight evaluations from such data for polysaccharides has been given (Fig. 14; see also [97]). Depending on the quality of the Rayleigh fringe data the improvement in precision compared with manual data capture systems would again appear to be highly advantageous for the determination of polysaccharide molecular weights. It is felt that this development could open up the possibility of the use of a whole series of analytical procedures which, although previously mathematically available, have been in practice unusable because of the severe requirements on the precision of the basic fringe data.

5.6 Applications

Compared to light scattering, examples of molecular weight determination using sedimentation equilibrium are not numerous for polysaccharides—and the situation is not likely to improve in the foreseeable future. Examples of applications to the determination of M_w data for a range of polysaccharides is given in Table 7 [98–106]. In general, results from sedimentation equilibrium are in good agreement with others, notably static light scattering

Table 7. Molecular weight of polysaccharide preparations from sedimentation equilibrium.

Polysaccharide	\bar{v} (ml/g)	$10^{-6} \times M_w^0$ (g/mol)	Experimental remarks	Ref.
Pullulan fractions:				
P100	0.60	0.095	low speed, Rayleigh	23
P800		0.76		
P1200		1.24		
Schizophyllan fractions:				
UR-28	0.62	0.13	low speed, Schlieren	98
D-24		0.23		
D40		0.48		
Lignin Fractions:				
L-1	0.66	0.23	ultrashort column, Rayleigh	99
L-3		0.41		
L-5		0.41		
Dextran T-500	0.61	0.50	low speed, Rayleigh	100
		0.42		25
DEAE-Dextran T-500	0.71			
Tomato pectins:				
green fruit	0.51	0.16		101
red fruit	0.50	0.096		101
Citrus pectin	0.57	0.090		108
Alginate, manucol DM	0.44	0.13		113
Galactomannans:				
Locust Bean T CWS	0.61	0.34		102
Y HWS		0.33		102
Guar	0.61	0.80		102
Glucomannan	0.61	0.28		103
<i>Pseudomonas aeruginosa</i>				
Immunotypes: 1	0.66	0.024	high speed, Rayleigh	104
4	0.62	0.017		104
7	0.62	0.019		104
β-Glucans (Barley)				
Clipper	0.62	0.29	high speed, Rayleigh	105
Commercial	0.62	0.16		
β-Glucans (Wheat)				
	0.62	0.098	low speed, Rayleigh	106
		0.28		
		0.23		
		0.10		

(for citrus pectin fractions [107]-108]; for pullulan fractions [23, 109, 110] and for dextran T-500 [111-113]). Where disagreement occurs it is normally associated with either clarity problems in light scattering or severe non-ideality in sedimentation equilibrium. Despite its lack of popularity it does provide absolute molecular weight data complementary to light scattering, and when used in conjunction with, for example, sedimentation velocity or intrinsic viscosity data provides also a powerful tool for conformational analysis. It is worth pointing out that the sedimentation equilibrium study of Kawahara *et al.* [23] has provided the basis of the commercially available pullulan standards which are now used worldwide for calibrating GPC columns (Section 7).

6. RELATIVE TECHNIQUES

These are so called because they require either (a) knowledge or assumptions concerning the conformation of the polysaccharide in solution, (b) calibration with the use of 'standard' polysaccharides of the same conformation and similar molecular weight to the sample whose molecular weight is being sought or (c) calibration using an absolute method coupled on- or off-line.

6.1 Viscometry

Viscosity is a molecular weight sensitive method that has been widely used most because it is rather easy to the experimentalist and does not require expensive instrumentation in its simplest form. Although the measurable quantities are easy to obtain, converting them to molecular weights and comparison with other samples is not always a straightforward task, and in many cases the use of intrinsic viscosity, $[\eta]$, as a hydrodynamic property is justified on its own without conversion to molecular weights. Experimental set-ups for determining viscosity range from the simple Ubbelhode-type viscometers, where the viscosity is evaluated from the flow rate for the Poiseuille flow [29], computer controlled capillary viscometers (e.g. the Schott Gerate 310/320 system), concentric cylinder viscometers (viscometers operating with a cone-and-plate or parallel plate geometries) through to the low shear concentric

cylinder viscometer originating from Crothers and Zimm [114, 115] (Cartesian Diver viscometer). Each of these has operational ranges for shear rates, ease of use, temperature control, sample volume, etc. The precautions needed to be taken in using $[\eta]$ in determining molecular weight will be stated here in terms of molecular properties rather than operational properties for each type of experimental setup. Whorlow [116], Ferry [117] and Kovar and Bohdanecky [118] give a more comprehensive presentation of the instrumental details.

Adding a known concentration of a macromolecule to a solvent changes the shear viscosity from that of the solvent, η_0 , to η . The intrinsic viscosity, $[\eta]$, is defined as (see, e.g. Yang [16] and Kovar and Bodhanecky [118]):

$$[\eta] = \lim_{c \rightarrow 0} (\eta - \eta_0)/(\eta_0 c) \quad (6.1)$$

and the viscosity of a solvent containing a finite concentration c of macromolecule can be expressed in Taylor expansion around η_0 in c :

$$\eta = \eta_0(1 + [\eta]c + k[\eta]^2c^2 + 0(c^3) + \dots) \quad (6.2)$$

where the first two coefficients have been explicitly stated in $[\eta]$ and $k[\eta]^2$, k being the Huggins constant. This identifies $[\eta]$ as the first-order perturbation on η_0 in polymer concentration. Equation (6.2) forms the basis for the experimental evaluation of $[\eta]$. $[\eta]$ can either be obtained as the intercept at the $c = 0$ axis of experimentally determined values of $(\eta - \eta_0)/(\eta_0 c)$ where the slope yields the Huggins constant, or alternatively, the intercept at $c = 0$ of $\ln(\eta/\eta_0)/c$ (the so-called Kramer plot), where the slope is $(1/2) - k$. Alternatively, the intrinsic viscosity can be obtained as $1/[\eta]$ from inverse Huggins and Kramer plots, the advantage being primarily that the evaluation of the Huggins constant does not depend on the value from the intercept. In both these approaches, the combined intercept for both Huggins and Kramer plots is preferred to that of using only one type of data evaluation. Equation (6.2) and the Taylor expansion of $\ln(\eta/\eta_0)$ can also be combined in other ways to obtain $[\eta]$, and one such expression at a finite concentration is [119]

$$\eta^* = \{2[(\eta - \eta_0)/\eta_0 - \ln(\eta/\eta_0)]/c^2\}^{1/2} \quad (6.3)$$

which, after truncation after the second term in the Taylor expansion of both series, becomes

$$\eta^* = [\eta]\{2[k' + (0.5 - k')]\}^{1/2} = [\eta] \quad (6.4)$$

which is insensitive to concentration. *c*. These two latter approaches are particularly useful in situations where a series of dilutions are difficult to obtain, i.e. in on-line column applications (see later). If such a one point concentration $[\eta]$ is, in fact, concentration dependent, this is reflected in the validity of truncating the Taylor expansion after the second term. The basis for using viscosity as a molecular weight sensitive method is the relation between the intrinsic viscosity (limiting viscosity number) and an average of the molecular weight. The dependence of the intrinsic viscosity of a homologous series of polysaccharides on the molecular weight is classically described in terms of the Mark-Houwink-Kuhn-Sakurada (MHKS) equation:

$$[\eta] = K' M^a \quad (6.5)$$

where K' and a are empirical parameters which are constants at a given temperature, for a specified solvent within each polysaccharide for a limited range of molecular weights. Equation (6.5) forms the basis for using viscosity to determine molecular weight. From a series of calibration substances which should be nearly monodisperse, determination of molecular weight and intrinsic viscosity yields estimates of K' and a for the given polysaccharide-solvent system. The coefficient a is a conformation sensitive parameter changing from 0.5 for randomly coiling polymers in θ solvents to 0.8 for polymers in good solvents, and increases with increasing chain stiffness attaining a value of 1.8 for the stiff rod conformation. This implies that the (a, K') parameters have a limited range of validity. To circumvent this limited validity of the parameters (a, K') and the MHKS equation, the intrinsic viscosity can be described in terms of the (helical) wormlike coil where the stiffness and the hydrodynamic diameter are the relevant parameters [120]. This latter description is valid ranging from the stiff rod limit to the random coil limit. In addition to the advantage of specifying only one set of parameters, the same type of parameters can also be used for the sedimentation coefficient and the translation diffusion constant [121]. The persistence length can also be used to calculate the radius of gyration obtained from light scattering.

As we have stated above, polydispersity is an inherent property of almost any polysaccharide preparation, and when dealing with an average measure, what type of average as well as deviations due to differences in molecular weight distribution should be indicated. The intrinsic viscosity of a polydisperse sample $[\eta]_w$, with a weight

concentration c_i of species i with molecular weights M_i and corresponding intrinsic viscosity $[\eta]_i$ is:

$$[\eta]_w = \sum c_i [\eta]_i / \sum c_i \quad (6.6)$$

Using the MHKS equation for this polydisperse sample defines the *viscosity average* molecular weight $M_\eta = \langle M_{a,0} \rangle$ (Eq. 2.5). For polysaccharide chains of intermediate stiffness corresponding to a molecular weight range with $a = 1$, the viscosity average molecular weight equals the weight average molecular weight. For $a > 1$, the viscosity average exceeds M_w , and does not correspond to any of those obtained by osmometry, or static light scattering. A more detailed discussion on the type of average provided by this formulation for different model molecular weight distributions is given by Bareis [122]. The M_η evaluated in terms of the helical wormlike coil corresponding to a molecular weight range where the MHKS does not describe well the $[\eta]-M$ relation in terms of a single set of a and K' coefficients is even more complicated. Nevertheless, the M_η for polydisperse helical wormlike coils has been formulated [123]. The total ionic strength in solution would affect the calibration parameters either using the MHKS equation [124] or the helical wormlike coil for polyelectrolytic polysaccharides [125], but as long as the unknown sample is characterized under the same solvent conditions as those used to obtain such calibration parameters, the polyelectrolytic nature would not introduce major errors in the determination of M_η . Chemical heterogeneity occurring in many classes of polysaccharide, e.g. alginates, locust bean gum and pectins, may cause problems in using such an indirect method. The calibration parameters (a, K') are reported to depend on the chemical composition for locust bean gum [2], and are expected to depend on the M/G ratio for alginates because of their difference in chain extension [126]. Differences in branching character for polysaccharides such as dextrans [127] and glycogen [128], between the calibration substances and the unknown substances may likewise affect the proper conversion to molecular weights. Thus, the chemical composition and the degree of branching for the material to be tested should resemble those of calibration substances to validate the use of such an indirect method. The theories relating the intrinsic viscosity to the molecular weight is formulated for the low shear Newtonian intrinsic viscosity, $[\eta]_{\dot{\gamma} \rightarrow 0}$, where $\dot{\gamma}$ is the shear rate. The onset of non-Newtonian behaviour depends on the

rotational relaxation time, τ_R , which depends on the molecular weight. Onset of non-Newtonian behaviour has traditionally not been utilized as an indirect method for molecular weight determination. We would only use τ_R to estimate an upper shear rate limit for obtaining the lower Newtonian plateau value. The rotational relaxation time for a macromolecule can be expressed in terms of its intrinsic viscosity and molecular weight [117]:

$$\tau_R = m[\eta]\eta_0 M/RT \quad (6.7)$$

where m is a slowly varying, conformation dependent parameter ($m = 1.15$ for stiff cylinders decreasing to $6/\pi^2$ for random coil type molecules [117]) and RT is the thermal energy. The onset of non-Newtonian effects occurs at about $\dot{\gamma}\tau_R = 1$. To ensure that we operate in the low-shear Newtonian plateau, the shear rate should be lower than $1/\tau_R$, or expressed in terms either of $[\eta]$ or M using the MHKS equation

$$\dot{\gamma} < RT(mK'^{-1/a}[\eta]^{1+1/a}\eta_0)^{-1} \quad (6.8a)$$

$$\dot{\gamma} < RT(mK'M^{1+a}\eta_0)^{-1} \quad (6.8b)$$

From the set of calibration data used to obtain the MHKS parameters, it is possible to obtain approximate upper limits for shear rates to ensure Newtonian viscosity using Eq. (6.8). However, rather than rely on such calculations, the ultimate way to ensure low-shear Newtonian behaviour is to measure $[\eta]$ as a function of $\dot{\gamma}$ in the range of $\dot{\gamma}$ suggested by Eq. 6.8 and extrapolate to $\dot{\gamma} = 0$.

The uncertainty in M_η resulting from operating in the non-Newtonian regime where shear rate effects are significant both when the calibration set and unknown samples are studied are rather obscure. If the molecular weight distribution for the unknown and calibration set of samples are identical, one might expect a rather small uncertainty in the final M_η estimate although the interpretation of the MHKS parameter a in terms of conformation is misleading. However, since τ_R is proportional to $M[\eta]$, it is more strongly weighted towards the heavier tail in a molecular weight distribution than $[\eta]$, and the onset of non-Newtonian behaviour can differ for samples of identical (low shear Newtonian) $[\eta]_{\dot{\gamma}=0}$, but with different polydispersity. With this in mind, it is recommended to check for non-Newtonian behaviour and ensure that the low-shear Newtonian plateau

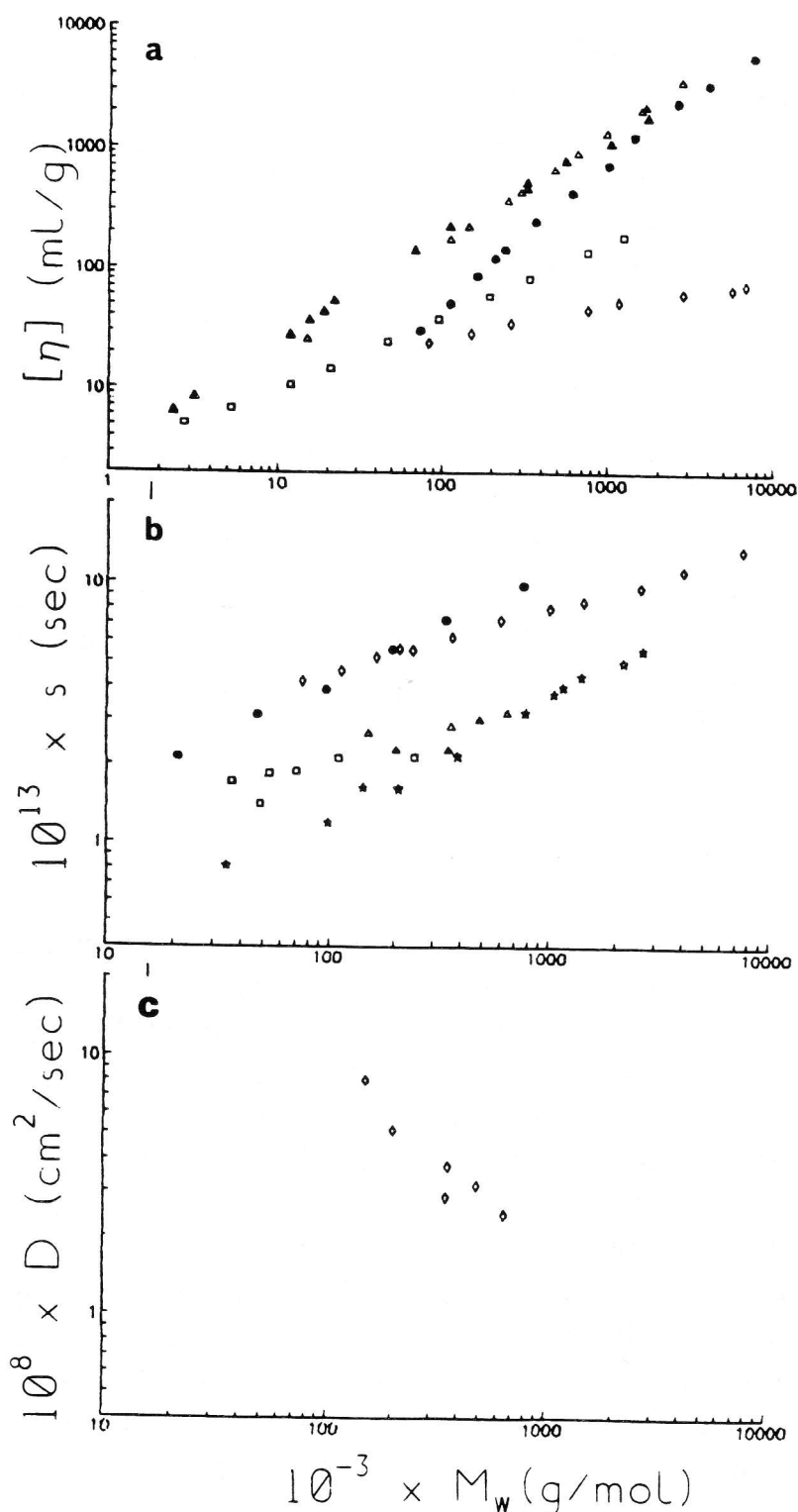


Figure 15. Double logarithmic plots of hydrodynamic data versus (weight average) molecular weight, M_w . (a) Intrinsic viscosity $[\eta]$ versus M_w : (\blacktriangle) hyaluronate [41]; (\triangle) alginate [130]; (\bullet) xanthan [129]; (\square) pullulan [23]; (\diamond) dextran [127]. (b) Sedimentation coefficient (infinite dilution value, corrected to water as solvent at 20.0°C) s versus M_w : (\square) citrus pectin [108]; (\bullet) pullulan [23]; (\diamond) xanthan [129]; (\star) amylose [130]; (\triangle) alginate [31]; (c) Translational diffusion coefficient (infinite dilution value, corrected to water as solvent at 20.0°C) D versus M_w : (\diamond) alginate [31].

is reached both for the calibration samples and the unknown samples.

6.1.1 Applications

Figure 15 shows double logarithmic plots of $[\eta]$ versus M for five different polysaccharides in aqueous solution. This figure is an example of a calibration plot which can be used to extract M from experimentally determined $[\eta]$. The intrinsic viscosity for the different polysaccharides ranges from dextran as the least molecular weight dependent, to pullulan, alginate and ending up with xanthan as the most molecular weight dependent. This is reflected in the value of the a —the MHKS coefficient. Some literature values of MHKS parameters together with the parameters needed in the (helical) wormlike description are compiled in Table 8 [131–134]. The a parameters reflect the chain stiffness as qualitatively discussed above and are shown in Table 8 not only to correlate with the persistence length, but also to the size scale used to evaluate a . Figure 15 [129–130] shows that xanthan is not well described in terms of the MHKS equation over the whole M range and that conversion of $[\eta]$ to M should only be done in the molecular weight range where the coefficients are valid, i.e. only interpolation and no extrapolation should be carried out. In such cases, the (helical) wormlike coil description [120] is valid over the whole M range and is clearly preferable to the MHKS equation.

Molecular weights have been reported based on experimentally determined intrinsic viscosities using the MHKS equation. Cael *et al.* [135], Moni *et al.* [136] and Rowe [137] all illustrate the simplicity of the method. Although relative variation in M obtained from such a method from polysaccharide preparations is clearly documented, the absolute values are strongly dependent on the actual (a, K') parameters. Comparison with absolute methods should be performed at some stage, or else the value of converting $[\eta]$ to molecular weights is quite limited. Lecourtier *et al.* [138] used the MHKS parameters determined from fractions of the same xanthan preparation to estimate M of several fractions of xanthan elution from column packed with non-porous material. They were able to resolve the molecular weight distribution of their xanthan material using the $[\eta]$ determined for the fractions and the average of the distribution corresponded well with the gross average of the material applied to the column.

Table 8. Mark-Houwink constants versus helical wormlike parameters.

Polymer	Solvent	Mark-Houwink constants			Helical wormlike coil parameters			Ref.
		I (M)	$K' \times 10^5$ (dl/g)	a	Molecular weight range (g/mol)	M_l (\AA^{-1})	q (\AA)	
NaCMC ^a	Aq. NaCl	0.005	7.2	0.95	1.4×10^5 - 1.1×10^6	48	231	23
	Aq. NaCl	0.01	8.1	0.92			184	(09)
	Aq. NaCl	0.05	19.1	0.82			110	19
	Aq. NaCl	0.2	43	0.74			80	49
	DMSO ^b					79		630
Amylose CMAm ^c	H ₂ O,					33.4		141
	H ₂ O,					82.7		131
	Aq. NaCl	0.1				194	1300 ± 200	56.5
Xanthan	0.01 N HCl						27 ± 5	129
	Aq. NaCl	0.75	2.4	0.96	4×10^6 - 1.5×10^7			
	NaCl	0.2	22.8	0.816	1.1×10^5 - 1.0×10^6			
Hyaluronic acid	0.5	31.8	0.777			190	1000 ± 200	20
							22 ± 3	132
							610	20
Schizophyllan	NaOH	0.01 N				40	45	134
							219	1800 ± 300
								22
Alginic	Aq. NaCl	0.01	0.48	1.15	$< 5.0 \times 10^5$		11	134
	Aq. NaCl	0.1	2.0	1.0	$> 1.0 \times 10^6$			56
	Aq. NaCl	1.0	9.1	0.87	1.1×10^3 - 2.7×10^6			124

^aSodium carboxy-methyl cellulose.

^bDimethyl selphoxide.

^cCarboxy-methyl amylose.

6.2 Sedimentation Velocity

We have already discussed one type of analytical ultracentrifuge technique: sedimentation equilibrium. Sedimentation velocity is perhaps a more familiar technique. However, unlike sedimentation equilibrium—and like intrinsic viscosity—it is a transport property: the rate at which a polysaccharide sediments under high gravitational fields is a function of its molecular weight *and* its conformation. Conventional schlieren optics are normally used to record the position of the sedimenting boundary [68] and an example is given in Fig. 16. From the rate of movement the sedimentation coefficient s_c , at a given concentration c , can be obtained. Two corrections are normally necessary (see, e.g. van Holde [21]). Firstly a correction to standard solvent conditions—normally water at 20.0°C. The second correction necessary is an extrapolation of s_c to zero concentration:

$$s_c \approx s(1 - k_s c) \text{ or equivalently } \frac{1}{s_c} \approx \frac{1}{s}(1 + k_s c) \quad (6.9)$$

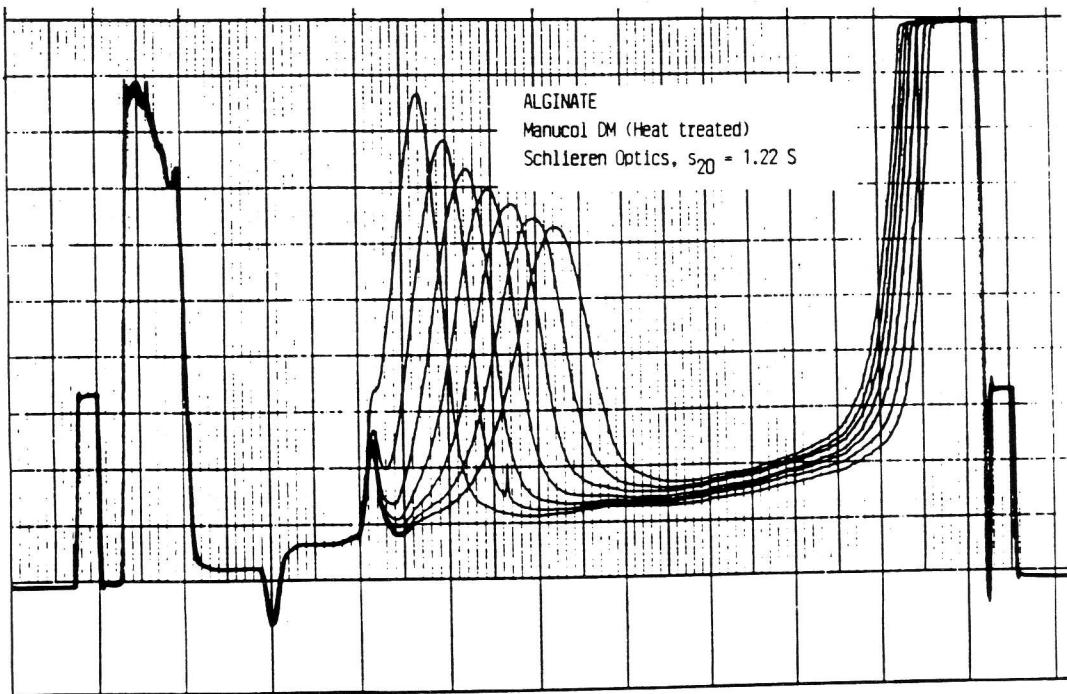


Figure 16. Schlieren boundaries for an alginate (heat treated manucol DM). Instrument: MSE Centriscan 75; monochromator set at 546 nm. Rotor speed = 49 000 rev/min. Temperature = 20.0°C. Loading concentration ~ 5.0 mg/ml. Solvent pH = 6.5; $I = 0.30$. Scan interval: 30 min.

The direction of sedimentation is from left to right.

where s is the 'infinite dilution' value and k_s the sedimentation concentration dependence regression coefficient. For non-spherical macromolecules normally the reciprocal value (Fig. 17) is extrapolated (see Rowe [139] for a discussion on this). It is also possible—at least in principle—to determine a distribution of sedimenting coefficients $g(s)$ from the shape of the sedimenting schlieren boundary (see, e.g. Fujita [63] and Hascall and Sadjera [140]) but besides concentration effects having to be taken into account this also requires a further correction for diffusion effects: some form of extrapolation to zero concentration and infinite time is required. A distribution $g(s)$ obtained after these criteria had been satisfied has been obtained by, for example, Iso *et al.* [141] for alginates.

Provided that the macromolecular conformation is known molecular weight data can be obtained from the sedimentation coefficient directly, and a distribution of molecular weights $g(M)$ from $g(s)$. For example the sedimentation coefficient has been related to the molecular weight by an MHKS type of relation:

$$s = K'' M^b \quad (6.10)$$

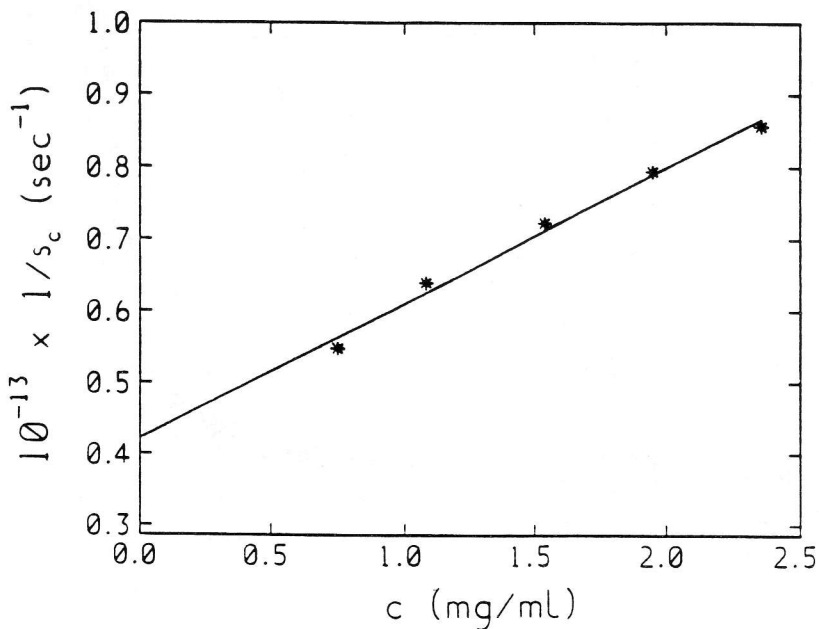


Figure 17. Extrapolation of the (reciprocal) apparent sedimentation coefficient s_c to zero concentration for (native) alginate manucol DM. Rotor speed = 49 000 rev/min. Temperature = 20.0°C. Solvent pH = 6.5; $l = 0.30$. All concentrations are true sedimenting concentrations (i.e. corrected for radial dilution effects). (From M. T. Anderson and S. E. Harding, unpublished observations.)

Thus if K'' and b are known then molecular weights can be specified. For a given polysaccharide series these constants can be found from a 'double-log' type of calibration plot for these materials where the calibrating molecular weights (normally isolated fractions of these materials) have been determined by an independent absolute technique, such as static light scattering or sedimentation equilibrium. Examples have been given in Fig. 15(b) for fractions of pullulan [23], pectin [108] and alginate [31]. By analogy with the MHKS plots from intrinsic viscosity (Fig. 15) the value of the exponent in Eq. 6.10 defines a conformation for the polysaccharide. For example, the value of 0.17 ± 0.07 for citrus pectin is consistent with an extended (rod) conformation and not a compact sphere or random coil. In some other cases—notably xanthan [129]—the conformation can change with increase in molecular weight (e.g. from an extended conformation at low molecular weight to a semiflexible coil at longer chain lengths).

There are other ways of obtaining absolute molecular weight data from sedimentation coefficients. One is to combine with translational diffusion coefficient data as described below (Section 6.3). The other is to combine with intrinsic viscosity data using a relation defined by Scheraga and Mandelkern [15], provided that the polysaccharide is not too asymmetric. This latter method relies on the insensitivity of the Scheraga–Mandelkern β function to shape [14, 16].

6.3 Translational Diffusion Coefficient Determination: Dynamic Light Scattering

As noted above (section 4) the advent of the laser, and the properties of high intensity, monochromaticity and collimation provided a major stimulus to the static light scattering method. The further property of high coherence provided the basis of a new type of scattering method in the 1960s [142]. Since macromolecules in dilute solution are subject to dominant Brownian diffusion, they impose a Doppler component on the otherwise almost monochromatic incident light. A spectrum analyser may be used to investigate such a wavelength spread and the diffusion coefficient may thus be determined. More usual is the study of the fluctuating intensity which arises from the beating of the components of different wavelength amongst themselves, and this is the basis of correlation techniques or 'dynamic light scattering'.

Dynamic light scattering comes under a number of different pseudonyms all meaning very much the same thing: quasi-elastic light scattering (QLS), photon correlation spectroscopy (PCS), intensity fluctuation spectroscopy (IFS). The principles of the technique are well described in a series of books [143, 144] and review articles [145–147], and the experimental aspects of application to biological macromolecules have also been considered in detail [148–150]. The principal feature of the apparatus illustrated schematically in Fig. 18 is a purpose-built digital correlator, and several instruments with this facility are commercially available e.g. Malvern 4700 equipment, Malvern Instruments, UK). For a system of spherical particles the (apparent) translational diffusion coefficient D_c , at a given concentration c , can be related to the normalized intensity autocorrelation function $g^2(t)$ via the relation [151]:

$$[g^2(t) - 1]^{1/2} = \exp(-D_c k^2 t) \quad (6.11)$$

where k is the Bragg wave vector. For a polydisperse system the (translational) diffusional coefficient will be a z-average [151]. For polysaccharides which are not in general spherical scatterers there will be a finite contribution to the autocorrelation function from rotational effects. This contribution can normally be eliminated by extrapolation of the normalized autocorrelation function to zero

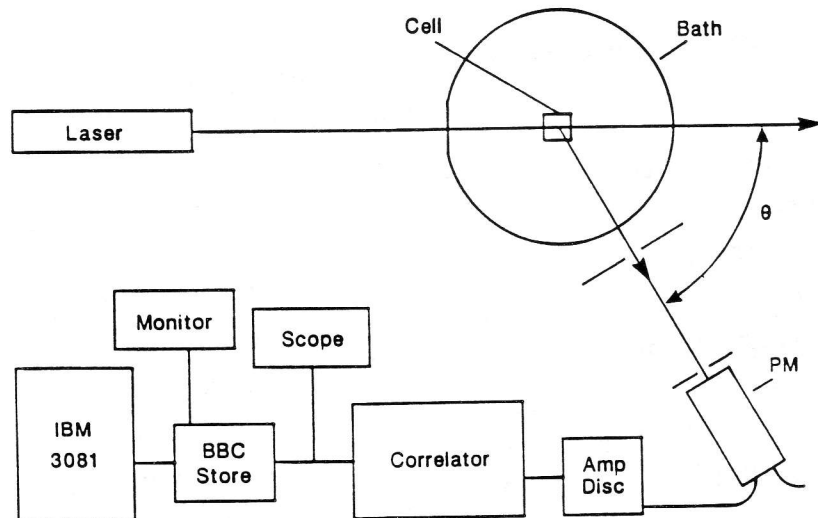


Figure 18. Schematic dynamic light scattering apparatus. Data from the digital correlator is captured using a microcomputer (in this example a BBC) and transferred to a mainframe computer for full data analysis (in this example the IBM 3081 at Cambridge). (From Ref. [148], with permission.)

angle [151], although at low angles artefactual contributions from any contaminating dust particles will be at their greatest.

By analogy with the sedimentation coefficient, D_c is conventionally corrected to standard solvent conditions—water at 20.0°C—and simple correction formulae are available [14]. The translational diffusion coefficient—like other hydrodynamic parameters—will be an apparent one, i.e. concentration dependent:

$$D_c = D[1 + (2BM - \bar{v} - k_s)c] \quad (6.12)$$

(see, e.g. [76]), where B is the osmotic pressure second virial coefficient and k_s is the sedimentation concentration regression coefficient—the same parameter as in Eq. (6.9). The ideal value, D , is normally found from a linear extrapolation of D_c to zero concentration.

The translational diffusion coefficient, by analogy with the sedimentation coefficient, can be used to obtain molecular weight information if the conformation is known. A similar MHKS type of expression exists to that for intrinsic viscosity and sedimentation velocity:

$$D = K'' M^{-\epsilon} \quad (6.13)$$

and a double logarithmic plot of diffusion coefficient versus molecular weight (the latter from static light scattering) for a series of alginates has been used to produce a calibration plot for these substances (Fig. 15c). The slope ($-\epsilon$) is again a function of conformation. The diffusion coefficient can also be used with the Scheraga—Mandelkern equation as discussed in Section 6.2 above although again we have no direct knowledge of its application. However, when combined with the weight-average sedimentation coefficient, s , this yields an absolute measure of the weight average molecular weight via the Svedberg equation:

$$M = (s/D)[RT/(1 - \bar{v}\rho_0)] \quad (6.14)$$

and has been applied to several alginates (e.g. Wedlock *et al.* [31]), giving values for the molecular weights in agreement with Zimm plot values.

We would like to stress that, just as for static light scattering problems of dust or supramolecular aggregates can lead to serious error with dynamic light scattering: the method has to be treated with extreme caution. Apparent agreement with results from SLS is not a sufficient criterion for correctness of results since contaminating

particles will produce results biased towards the spuriously high molecular weights in both cases. The problems with dynamic light scattering have been considered in detail by Comper *et al.* [152]. These latter workers have proposed that boundary spreading in the ultracentrifuge may in certain cases be preferable, but this too is not without difficulties for polydisperse materials. An estimate for the molecular weight from the Svedberg equation for guar and locust bean galactomannans, where the translational diffusion coefficient was measured by the boundary spreading in the ultracentrifuge, has been given by Sharman and Richards [153]. The results obtained (0.66 and 0.32) $\times 10^{-6} \text{ cm}^2 \text{ s}^{-1}$ are in reasonable agreement with those from sedimentation equilibrium (see Table 7), but much lower than that from light scattering [154]. In a later study good agreement between the two techniques was obtained for dextrans [155]. It is also possible to define distributions of diffusion coefficient and hence, if the parameters of Eq. (6.13) are known, a distribution of molecular weights [55], and an example of application to a bacterial polysaccharide has been given by Chu *et al.* [8]. Software packages are commercially available permitting these calculations on microcomputers. These analyses, however, besides being subject to the usual problems of solution of multi-exponential equations without constraints, do not in general take into account effects of non-ideality, which will be considerable as noted above for concentrations ($c \gtrsim 1.0 \text{ mg/ml}$).

7. GEL PERMEATION CHROMATOGRAPHY

Knowledge of the molecular weight distribution, and not only molecular weight averages as provided by osmometry or classical light scattering, is needed to give a detailed description of molecular weight properties of a certain polysaccharide sample. As discussed earlier (Section 1), the polydispersity of polysaccharide preparations might yield point-average molecular weights obscuring molecular weight tails in either direction, which is of significance in certain applications such as for the use of carrageenans as food additives.

Among the techniques available to provide information about the whole molecular weight distribution, calibrated gel permeation chromatography (GPC) has been—for several years—the most

popular in the field of polysaccharides. When the stationary phase in the column is carefully selected to the problem at hand, and when appropriate calibration methods and data handling procedures are applied, this approach has the potential of resolving the 'true' molecular weight distribution. However, there are several experimental hurdles to overcome to meet this ultimate goal. We have chosen to give a practical and applied approach in using GPC to characterize carbohydrate polymers and, for this reason, we will not go into detail of the separation mechanisms involved which can be found in textbooks [156, 157]. However, a brief account of fundamentals necessary to understand the separation process relevant to polysaccharides is provided. This is necessary as a basis for the discussion of calibration methods, data handling procedures, etc., which can be found elsewhere [157, 158].

In GPC, components migrate through the column matrix with different velocities and consequently elute at different times after injection. The difference in migration velocities occurs due to retention of the molecules by the stationary phase. Ideally, the retention of the molecules depends on the hydrodynamic volume of the molecules relative to the accessible pore volume for the given hydrodynamic volume, v_h . For molecular species with v_h in excess of the largest available pore size of the stationary phase, separation based on accessibility of interparticle pores occurs. This is also referred to as hydrodynamic chromatography (flow-field fractionation) and occurs essentially due to steric exclusion of the polymer molecules from the particle walls. This latter retention mechanism is utilized for high molecular weight polysaccharides with very large hydrodynamic volume [138, 159, 160]. In conventional GPC the hydrodynamic chromatography effect is one mechanism leading to band broadening [157].

Separation mechanisms not governed by the size of the molecules will tend to decouple the molecular size-migration velocity relation, and the experimental elution profile will not reflect differences in size. Such non-size separation mechanisms can be a result of, for example, charge effects and adsorption. These phenomena and the necessary precautions to minimize their influence are described by Barth [158], and have recently been reviewed when using GPC to characterize polysaccharides [161]. In conventional GPC, a small applied amount of a monodisperse polymer ideally elutes as a sharp peak at an elution volume determined by its characteristic migration

velocity. In practice this is not observed due to different broadening mechanisms. This implies that an applied Dirac- δ molecular weight profile (this is the mathematical representation of a monodisperse polymer) elutes as a broadened band where the peak position represents the most probable molecular weight and the width of the distribution represents the system (column, tubes, valves and detector) impulse response. An experimental elution profile obtained from a concentration sensitive detector can be converted to a molecular weight distribution provided that the column used is properly calibrated for the polysaccharide under experimentation. The most complete approach requires that the experimental elution profile is first corrected for system dispersion, in which calibration data for dispersion as a function of elution volume is required, and, secondly, that the corrected chromatogram is converted to a molecular weight distribution using a calibration equation relating the elution volume to molecular weight. Before we present different ways of calibrating columns, we first deal with the selection of column materials in view of polysaccharides to be studied.

7.1 Selection of Column Material

Manufacturers of commercial column materials provide separation ranges for their different products mainly in terms of separation ranges valid for globular proteins or dextrans. It is well documented in the polysaccharide literature that most polysaccharides have more extended conformations than the highly flexible and branched dextran molecule, and certainly more extended than the compact conformation of globular proteins. The hydrodynamic volume of the stiffer polysaccharides is therefore larger than for the corresponding molecular weight of dextran as illustrated in Fig. 15 where the intrinsic viscosity of five different polysaccharides are shown versus molecular weight. The separation range is therefore expected to differ from that of dextrans and the guidelines given by the manufacturer for dextrans are not generally reliable for the stiffer polysaccharides. It is a necessary requirement that the molecular weight range in the sample is within the separation range for the column material to be able to separate on molecular weight and thereby obtain the molecular weight distribution.

Table 9. Approximate molecular weight (in kDa) separation ranges for pullulan, alginate and xanthan on different columns.

MHKS constants a K' (ml/g)	Globular proteins	Dextran	Pullulan	Alginate	Xanthan
Pharmacia: Sephacryl high resolution					
S-100 HR	1-100	1-80	1.5-70	1.5-35	1.5-35
S-200 HR	5-250	2-400	3-300	2.5-125	2.5-125
S-300 HR	10-1500	10-2000	11-1250	8-400	9-400
S-400 HR	20-8000	40-20000	40-10000	20-2500	20-2000
S-500 HR					
Sephadose					
6B/Cl-6B	10-4000	10-1000	11-700	8-250	8-250
4B/Cl-4B	60-20000	30-5000	30-3000	20-800	20-700
2B/Cl-2B	70-40000	100-20000	90-10000	45-2500	45-2000
Superose 12	1-300	1-100	1.5-90	1.5-45	1.5-45
Superose 6	5-5000	1-1000	1.5-700	1.5-250	1.5-250
Bio-Rad: Biogel					
TSK-40 (G 4000 PW)	1-700	1.5-500	1.5-200	1.5-200	1.5-200
TSK-50 (G 5000 PW)	10-2000	11-1300	8-400	8-400	8-400
TSK-60 (G 6000 PW)	100-20000	90-10000	45-2500	45-2500	45-2000

Based on the principle of universal calibration (see below) and reported constants in the MHKS equation (Eq. 6.5, Table 8), separation ranges for different column materials have been converted from those for dextrans to other polysaccharides (Table 9). A more comprehensive tabulation is given by Barth [158]. The actual values should be considered as only approximate guides because they depend to some extent on the actual values of the MHKS parameters both for dextran and the other polysaccharide (and they have a limited range of validity as stated above, Section 6.1, which is not met in some of these calculations). Table 9 demonstrates that the separation ranges become narrower the stiffer the polysaccharide (larger MHKS exponent), and particularly that the upper limit of the separation range is lowered by up to a decade from that for dextran. The three polysaccharides considered in Table 9 were selected partly because they are among the most studied, partly because pullulan represents a widely used calibration standard and, lastly, because they span a large range of chain stiffnesses. When either sample average M_n or M_w are known, columns should be selected to resolve M from below $0.2 M_n$ and up to $5 M_w$ or even a larger range. A proper determination of the void volume, i.e. the elution volume for totally excluded polysaccharides, using a very high molecular weight preparation, and the total volume, using a low molecular weight compound such as glucose, is necessary to ensure that the chosen column(s) is able to resolve the molecular weight distribution. By combination of columns in series it is possible to improve the linearity of the separation range and the effective separation range when the pore size distributions of the two columns are properly adjusted to each other [162]. This will, firstly, diminish the resolution and, secondly, not increase the upper resolution limit of column with the largest resolution limit. This upper resolution limit is one of the limiting factors in characterization using GPC of high molecular weight polysaccharides such as xanthan, scleroglucan and others. The selection of column material is in many cases balanced by the two mutually excluding aims of having the highest possible resolution and a wide as possible separation range.

7.2 Calibration using Standards

The earliest attempts to convert chromatograms to molecular weight distributions were based on calibration procedures where standards, either synthetic polymers or dextran, were utilized.

For molecules eluting between the void and total volume, the molecular weight is adjusted to a polynomial in elution volume, V :

$$\log(M) = \sum_{i=0}^N \alpha_i V^i \quad (7.1)$$

A linear calibration equation ($N = 1$) will for many instances fit the data adequately, whereas non-linearities occurring in particular close to the void and the total volume can be taken into account incorporating higher order terms. The coefficients α_i can be determined either based on the peak position of near-monodisperse fractions covering the whole molecular weight range separable by the column/solvent system. The peak position method is considered as one of the best methods to obtain calibration equations [157]. In this context it should be noted that the peak position method is not affected by system dispersion if it is described in terms of a Gaussian band. However, one should be aware of what kind of average is known for the calibration standards and the type of detector used (concentration sensitive, number of particle sensitive or other). Once the coefficients in Eq. (7.1) for a given column–polysaccharide–solvent system have been determined, experimental ‘true’ chromatograms can be converted to molecular weight distributions.

The experimental limitations in applying the peak position–off-line calibration method are mainly in the experimental uncertainty in the molecular weight and peak position determination of the standards. Error propagation to the M averages of the unknown sample have been studied using computer generated data [19, 157] and show that the relative error is larger the higher the molecular weight moment.

Calibration using dextran fractions and then estimation of molecular weight distributions of other type of polysaccharides is the simplest, although not truly correct, implementation of such an approach. When using columns calibrated with dextran fractions to determine molecular weight distributions of pectins [163], hemicellulose [164] or other polysaccharides, the molecular weights obtained should be regarded as *equivalent* dextran molecular weights rather than absolute for the substance in question. Or, in other words, the unknown samples elute at a volume corresponding to the specified molecular weight of dextran. Table 9 (and Fig. 19) show that the actual molecular weight for other substances is expected to differ from that of dextran and the absolute values of these other polysaccharides should, in such cases, be treated with some caution.

The calibration using the peak position method is limited by availability of homologous fractions of the polysaccharides studied. Off-line calibration in these cases can be obtained either using a broad molecular weight standard or based on the principle of universal calibration. Calibration using a broad molecular weight standard is affected by the system impulse response. Correcting for this line broadening can be taken into account in obtaining the calibration equation assuming that the δ is transformed into a symmetric Gaussian band, using the 'GPCV2' method [165], or even skewed column dispersion, using the 'GPCV3' method [157, 166].

Calibration using broad molecular weight standards can be performed either based on the integral molecular weight distribution or using specific, known averages of the standard. The integral molecular weight distribution method requires that the complete molecular weight distribution is known. This method is scarcely utilized in the field of polysaccharides and we therefore omit any further description of it. The latter is recommended when the column material is selected to yield a linear calibration equation because, thus far, it has been limited to assuming a linear calibration equation, i.e. $N = 1$ in Eq. (7.1). Both the integral method and the peak position method based on the linear calibration equation ($N = 1$ in Eq. 1) are presented in detail elsewhere [157].

Off-line universal calibration is based on the concept of use of the hydrodynamic volume of non-homologous series of polymers. The hydrodynamic volume can be expressed as the product of the molecular weight M and intrinsic viscosity $[\eta]$ and the calibration equation has the form:

$$\log(M_n[\eta]) = \sum_{i=0}^N \beta_i V^i \quad (7.2)$$

where β_i are adjusted based on the calibration data. For slightly polydisperse polymers it is the M_n and the elution volume for the M_n that should enter this calculation [167]. When the universal calibration approach is utilized, additional information about the polysaccharide must be provided to obtain molecular weight distributions. This can be the a and K parameters in the MHKS equation (Eq. 6.5). The principle of universal calibration is shown to work well for a limited range of chain stiffnesses, whereas extremes

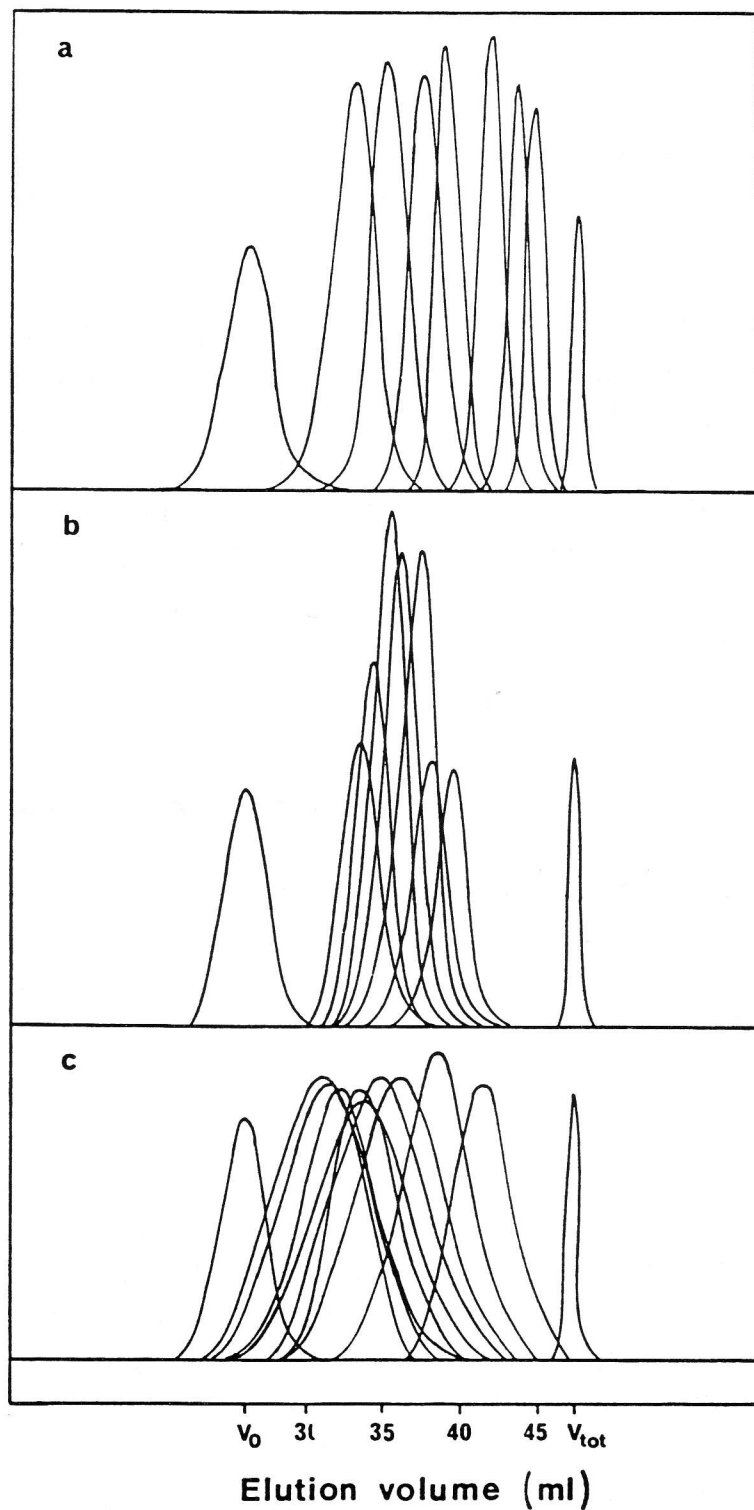


Figure 19. GPC elution profiles of narrow fractions of pullulan (a), alginate (b) and (1-3) (1-4)- β -D-glucans (c) separated on TSK-gel G 5000PW and G 6000PW.

such as globular proteins and stiff rod-like conformations do not conform to this principle [168]. The use of universal calibration for polysaccharides should therefore be tested prior to application, at least for stiff chain polysaccharides in combination with more random-coil like examples.

The universal calibration concept has been utilized [169] to determine the molecular weight distribution of, for example, hyaluronic acid, and values for M_w obtained from the GPC elution profiles were within reasonable agreement with that determined by light scattering.

Such 'off-line' calibrated columns have been widely used for polysaccharides. As an illustrative example we present some elution profiles obtained on TSK columns for several fractions of pullulan, alginate and β -D-(1-3), (1-4)glucans [169a]. The void and total volume were determined using a high molecular weight xanthan fraction and glucose respectively. Figure 19 shows that the complete elution profile of each of the fractions elute between the void and total volume, that most of the fractions elute as near-symmetric Gaussian shapes, and the range of molecular weight in the fractions span a rather large range.

7.3 Calibration for System Dispersion

The column dispersion smears out any sharp peaks and the experimental chromatogram $F(V)$ can be expressed as the convolution of the true chromatogram $W(V)$ and the system dispersion according to Tung [170]

$$F(V) = \int_{-\infty}^{+\infty} W(Y) G(V - Y) dY \quad (7.3)$$

A deconvolution method can in principle be used to obtain the true chromatogram when the system dispersion function is known. However, it has been a problem for a long time to avoid oscillations in the true chromatogram close to sharp peaks (high frequency components), and analytical approaches where the Gaussian shape ('GPCV2') or skewed Gaussian ('GPCV3') are assumed for the dispersion function are most prevailing. All these methods rely on experimentally determined values describing the system dispersion. Assuming that the system dispersion is adequately represented by a Gaussian function, and that the column calibration equation can be piecewise approximated by a two-parameter fit [$\log(M) = (\alpha_0 + \alpha_1 V)$ or $N = 1$ in Eq. (7.1)], estimates of system dispersion parameters can be obtained. Note that different α_i values can be used for different calibration substances covering

non-overlapping regions of V . Under these assumptions [171], 172], the ratio between M_w and M_n depends on the same ratio calculated from the uncorrected chromatogram, and the standard deviation σ is the system dispersion function:

$$M_w/M_n = (M_w/M_n)_h \exp(-\alpha_i^2 \sigma^2/2) \quad (7.4)$$

where $(M_w/M_n)_h$ is the polydispersity calculated from the uncorrected experimental chromatogram and calibration equation. It is not corrected for system dispersion and thus reflects an increase in the polydispersity index. This is valid irrespective of the complexity of the molecular weight distribution of the sample used to calibrate σ as long as the above stated assumptions are satisfied. Corrections for instrumental spreading are not widely applied and represent in some cases minor corrections for narrow molecular weight standards such as pullulan (0.8–1.9% correction [173]). The correction is more significant for the resolution of the molecular weight distribution than for actual values of M_n , M_w and M_z calculated from the chromatograms.

8. MAXWELL'S DEMON: COMBINED FRACTIONATION/ABSOLUTE APPROACHES

Interpretations of the data from the ‘absolute’ techniques we have discussed above—osmotic pressure, sedimentation equilibrium and total intensity light scattering—are all coloured by problems of polydispersity of polysaccharides. This polydispersity problem is largely dealt with by sedimentation velocity and gel permeation chromatography which can, if appropriate conditions are chosen, provide a satisfactory fractionation or resolution of the components of different molecular weight, but insofar as molecular weight determination is concerned, these are only ‘relative’ techniques—the separations are dependent on conformation as well as molecular weight. The revolutionary step has been to use a ‘fractionation’ technique as a ‘Maxwell’s Demon’ in conjunction with an absolute molecular weight technique to give absolute molecular weight distributions. ‘Maxwell’s Demon’ was in its original conception ([174]; see also Klein [175]) an intelligence able to separate gas molecules moving at different velocities. By analogy, in system of

molecules polydisperse by weight (as opposed to velocity) this 'Demon' is able to separate molecules of different weight prior to analysis. In the case of polysaccharides this Demon is not an 'intelligence' but either GPC or sedimentation velocity. It is fair to say that this particular 'Maxwell Demon' has provided a major impetus to the determination of molecular weight distributions, and in the case of on-line GPC/light scattering has largely solved the dust problem. These methods are generally valid provided that non-ideality effects are properly taken into account and provided that the polysaccharide system is not reversibly associating: samples will simply redistribute after fractionation leading to serious errors of interpretation. The other complication that can occur is that if

Table 10. Combined fractionation/absolute techniques for molecular weight distribution analysis.

Fractionation technique	Absolute technique	On/off line	Polysaccharide	Ref.
GPC	sedimentation equilibrium	off	alginate manucol DM	113
			citrus pectin	108
			T-500 dextran	100
GPC	light scattering (total intensity)	off	citrus pectin	107
			<i>i</i> -carrageenan	176
GPC	low angle (total intensity)	on	κ -carrageenan	177
	light scattering		xanthan	178
			dextrans	179
			inulin	183
			sinistrin	183
			scleroglucan	29
			guar	181
			amylose	182
			amylopectin	182
			starch	182
			glycogen	182
			cellulose	183
GPC	multi-angle (total intensity)	on	hyaluronic acid	184
	light scattering		T-500 dextran	111
SFFF	light scattering (evaporative)	on	P-800 pullulan	111
			dextran	187

the polysaccharides are copolymers the observed distributions may be influenced by polydispersity in composition as well as molecular weight. Polydispersity in composition will be manifested by polydispersities in partial specific volume for sedimentation equilibrium and polydispersity in density increment for total intensity light scattering, as indicated in Section 2.1 above. In Table 10 [176–187] we have cited the five main approaches involving either off-line or on-line calibration of GPC (principally) or sedimentation velocity. We will now consider them in a little more detail.

8.1 Off-line Calibration of Gel Permeation Chromatography by Sedimentation Equilibrium

This was considered implicitly by Wasteson [188, 189] for chondroitin sulphate fractions, by Kawahara *et al.* [23] for pullulan fractions and has been considered in detail by Ball *et al.* [113]. For example, the idea is to isolate several (typically five or six) fractions of narrow bandwidth from the column and determine their molecular weights using ultrashort column low speed sedimentation equilibrium in multi-channel cells (to accelerate the acquisition of data) [113]. This defines a calibration plot of $\log_e M$ versus V_e which can be used to define a distribution of molecular weights from the GPC elution profile.

8.2 Off-line Calibration of Gel Permeation Chromatography by Total Intensity Light Scattering

This follows almost exactly the same sort of principle as Section 8.1., except that *Zimm plot* analyses are performed on each of the fractions (see, e.g. Ekstrom *et al.* [176]). This also facilities the determination of distributions of size (via R_G) and a check on variation of the second virial coefficient B . It is generally more difficult to perform than 8.1 because of the larger amounts of material required and because of the usual dust problems although the fractionated material itself will be ‘cleaned’ by the GPC. For example, for the case of a series of citrus pectin fractions, results from this procedure are in excellent agreement with those from sedimentation equilibrium [108].

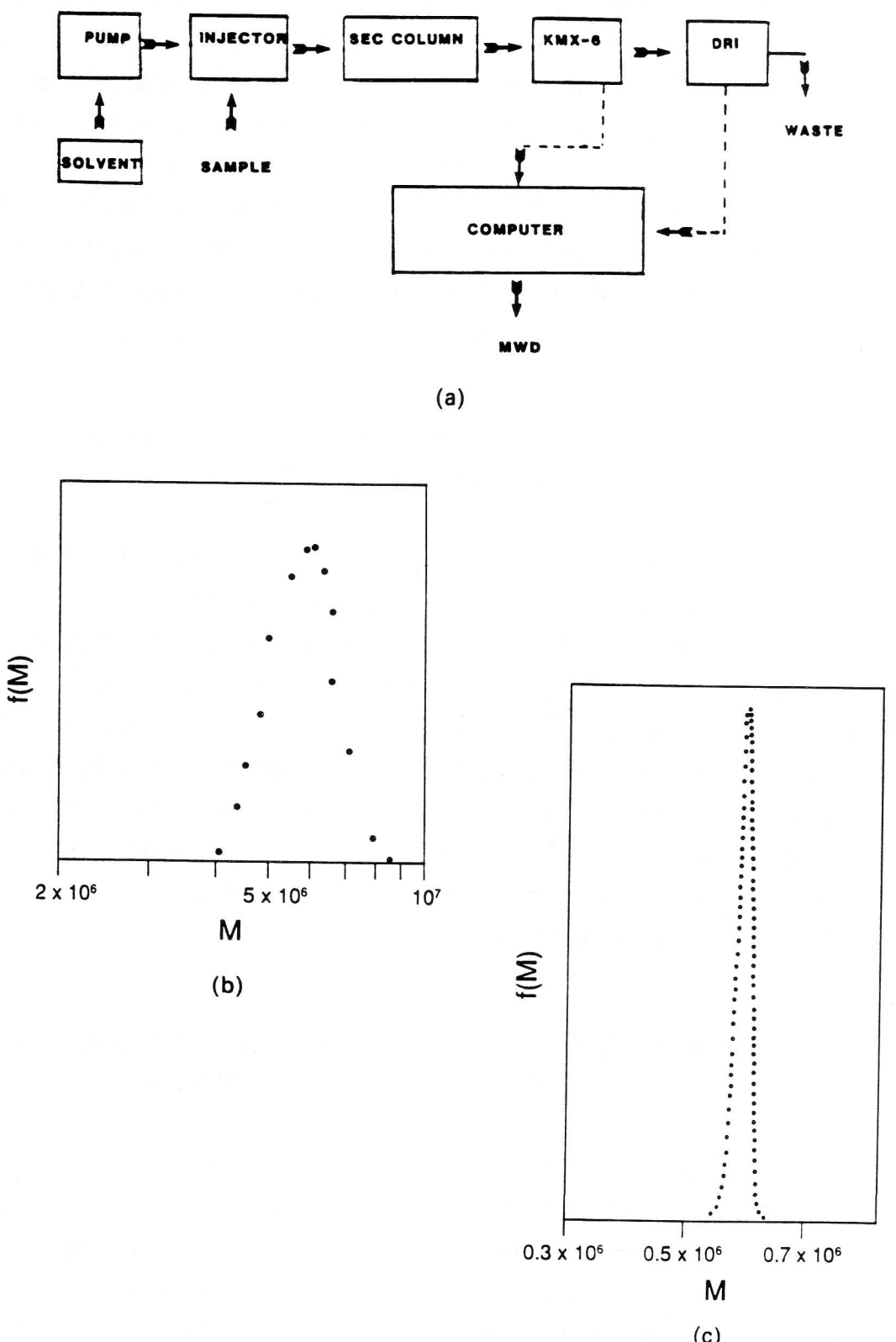


Figure 20. GPC(SEC)/LALLS for molecular weight distribution determination. (a) Schematic [181]. (b) Molecular weight distribution for schleroglucan [29]. (c) Molecular weight distribution for hyaluronic acid [184].

8.3 On-line Calibration of Gel Permeation Chromatography by Low Angle Laser Light Scattering

Off-line calibration methods tend to be time-consuming. Kaye and Havlik [190] announced in 1973 the revolutionary approach of installing a low angle light scattering detector 'on-line' with a GPC column-differential refractometer arrangement. The device, originally available from Beckman Instruments (Palo Alto, Ca) is now available as the 'KMX-6' (Milton Roy, Florida) and Fig. 20(a) gives a simple outline of the method. It has been applied to a wide range of polysaccharides as Table 10 illustrates. Figure 20(b) and (c) give two examples of distributions obtained in this way for scleroglucan and hyaluronic acid, respectively. One of the chief difficulties is thermodynamic non-ideality. The second virial coefficient, B , is normally determined separately on unfractionated material with either accurate dry weights or a properly calibrated refractometer for concentration measurement. B is normally taken as constant for given fractions from the polysaccharide and provided that the concentrations can be recorded on line with the GPC/LALLS using the refractometer, non-ideality can be allowed for. The other assumption that is made is that the angle is low enough that the angular dependence is totally eliminated.

8.4 On-line Calibration of Gel Permeation Chromatography by Multi-angle Laser Light Scattering

With low angle light scattering, even on samples directly from a GPC column, there is still the lingering doubt over residual bits of dust, small pieces from the column, etc., still appearing in the scattering cell, and also problems of 'flares' from the walls of the cell. The appearance of GPC/multi-angle laser light scattering (Dawn-F, Wyatt Technology, Santa Barbara) appears to represent a considerable improvement, although as yet there are few examples of application to polysaccharides (Table 10). Figure 21 gives the calibration plot and (cumulative) molecular weight distribution for a Pullulan fraction P-800. The results are in good agreement with data from, for example, sedimentation equilibrium [23]. The same attention to thermodynamic non-ideality noted in Section 8.3 above has to be applied. It is also possible to obtain from these types of analyses distributions of root mean square radii, R_G values,

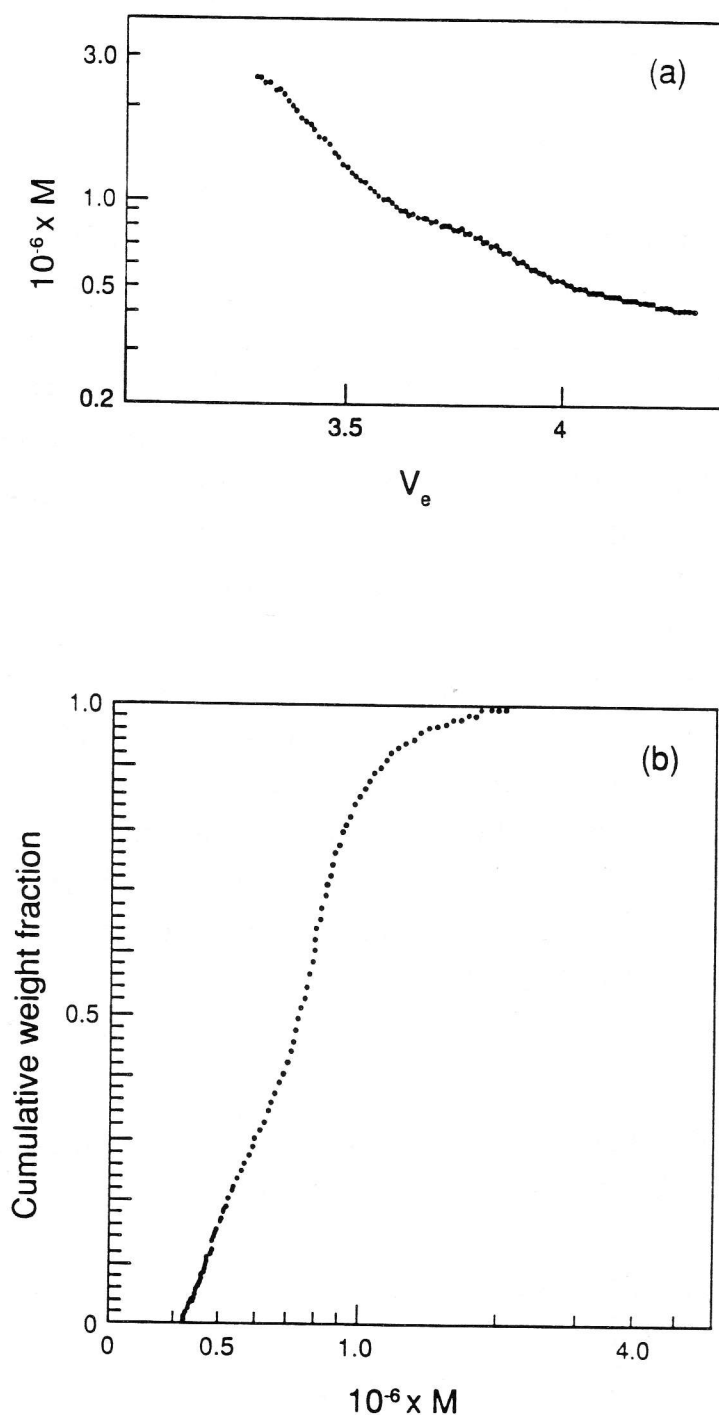


Figure 21. GPC (SEC)/MALLS for molecular weight distribution determination. Data obtained from the Dawn Model F instrument (Wyatt Technology, Santa Barbara, Calif.) coupled to Waters HPLC equipment, on Pullulan P-800. (a) Calibration plot of log molecular weight versus elution volume. (b) Distribution of molecular weight (expressed as a cumulative weight fraction). (From Ref. [111], with permission.)

since simultaneous measurements at multiple angle are being made. It is therefore possible to define very rapidly a plot on double logarithmic scale of M_w versus R_G , which as noted above defines a conformation for the polysaccharide. It is not unreasonable to say that the appearance of GPC/MALLS could represent one of the most significant developments for the determination of absolute molecular weight distributions of polysaccharides.

8.5 On-line SFFF/Light Scattering

Sedimentation field flow fractionation (SFFF) is a sedimentation velocity type of process performed in a modified preparative type of ultracentrifuge. These are commercially available (DuPont Instruments) and consist essentially of on-line pooling through suitably designed radial channels in the rotor system. SFFF achieves much the same goal as GPC but is better suited for larger macromolecules where GPC separations are generally poor (see Section 1). Oppenheimer and Mouray [187] have built an 'evaporative light scattering detector' on-line to the SFFF channels and obtained a molecular weight distribution for a dextran (Fig. 22). The possibility of incorporating a MALLS detector instead is now being considered (P. Wyatt, personal communication).

Viscosity detectors are also becoming increasingly popular [119, 191] but since these yield only a relative measure of molecular weight they are inferior to those detectors which give absolute

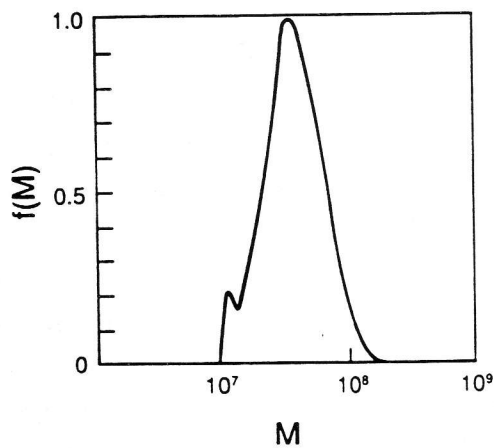


Figure 22. Molecular weight distribution of a dextran obtained from SFFF coupled to an evaporative light scattering detector. (From Ref. [187], with permission.)

molecular weights when molecular weight distributions are concerned. The main advantage of using a viscosity detector to a GPC column in combination with a M detector is that it provides estimates of η , M and c for a range of fractions as they elute from a column, thereby obtaining a calibration plot analogous to Fig. 15(a) for the polysaccharide in question [191]. However, as these on-line viscosity detectors are usually of the capillary type, there might be significant deviations from low-shear Newtonian viscosity for high molecular weight polysaccharides (Section 6.1).

9. OTHER METHODS

In addition to the techniques presented in some detail above, there are a few others that should be described briefly. End group analysis is one such technique. If the molecular weight of a macromolecule should be determined through a group analysis, it is required that the polymer contain a known number of determinable groups per molecule. For polysaccharides such analyses are, in practice, limited to end groups and the method is referred to as end group analysis. Since the method counts the number of molecules in the sample, it is M_n that is determined. The type of groups that can be determined depend on the type of polysaccharide, and therefore no general method can be given. However, linear polysaccharides have a non-reducing end which is suitable for derivatization, e.g. by a fluorescent or radioactive agent. Nuclear magnetic resonance (NMR) may also yield specific signals from end groups which can be quantified. The latter method is, however, limited to rather low molecular weights (10 000 g/mol or less) due to the signal-to-noise ratio in the spectrum.

Any physical measure which shows a molecular weight dependency could in principle be used to characterize molecular weight. The greater the dependency (i.e. larger exponent in a power law relationship), the better the potential resolving power. Tomka and Vancso [19] have listed some mechanical properties of polymer molecules in the melt concentration regime which may be used to characterize molecular weight. So far, these melt properties have seen limited use in obtaining molecular weights of polymers and in the case of polysaccharides (which in many cases deviate

significantly from the underlying theories as suggested to measure molecular weight) no reports on using this kind of approach are known to us. The measured molecular weights are also affected by polydispersity in a somewhat different way than, for example, obtained by classical light scattering or osmosis. This may hamper the correlation of data obtained on the same sample using different techniques, but has also the potential of gaining more information as the average is weighted to other ranges in the molecular weight distribution than, for example, M_n obtained from osmometry.

Tomka and Vancso [19] also discuss the potential of applying the correlation between the random polymer coil–stretch transition and the effect of this molecular process on the elongational viscosity as a molecular weight sensitive method. This concept is explored by Keller *et al.* [192–195]. Polymer molecules exhibiting entropic nature can be induced to go from the coil form to the fully stretched form in an elongational shear field provided that the elongational strain rate, ε , exceeds $1/\tau$ and the residence time of the polymer in the high strain rate field is sufficient for the transition to occur. The characteristic relaxation time τ was predicted to be identical to the first relaxation time in a free draining or non-draining coil. Applying this technique to molecular weight determination of polymers requires calibration using nearly monodisperse polymer molecules of the same chemical composition as those to be investigated. Deviation from entropic dominated nature would make data interpretation difficult in distinguishing between effects of polydispersity and effects of chain stiffness and therefore ambiguous. This is exemplified by Pfeiffer *et al.* [196] for xanthan. The feature that sets this experimental approach apart from the previous ones is that it is sensitive to molecular weight and molecular weight distributions in the range from 10^6 and upwards, where the available packing materials for GPC clearly have their limitations (Table 9). In spite of the experimental hurdles and possible ambiguous interpretation, this technique should be worth exploring for characterizing polysaccharides. The high molecular weight limit in the microrheology–elongational shear field technique corresponds to the value where the critical elongational strain rate needed to induce the coil–stretch transition exceeds the one to induce chain scission [192]. For such high molecular weights another technique also based on the polymer molecule relaxation times can be employed.

For native DNA of different origins having molecular weights in the range 10^7 to 10^{11} g/mol, molecular weights have been determined using the creep recovery phenomena as observed in a low shear Cartesian diver viscometer [197]. In this molecular weight range, the structural features of DNA with a persistence length of about 50 nm are adequately represented by Gaussian chain models. For the creep recovery after controlled upwinding of the molecules, the movement of the Cartesian diver is governed by the relaxation of ensembles of individual polymer molecules in the limit of infinite dilution. This type of decay can be analysed to yield the molecular weight. The main experimental difficulty with such a technique is in the handling of the high molecular weight macromolecules without inducing any shear damage. For DNA this was accomplished by lysing the cells directly in the measurement cuvette. The technique can be extended to the characterization of polysaccharides. For example, raw extracts of alginates from *Aschophyllum nodosum* fruiting bodies are observed (Smidsrød, unpublished observation) to cause creep recovery in a Zimm type viscometer which indicate that they may contain very high molecular weight polysaccharides.

The rotational relaxation time can also be measured using either shear flow birefringence or electrically induced birefringence (see, e.g. Morris [198]). To our knowledge these methods are not widely used to determine molecular weights of polysaccharides, and since they are relative methods, we will not consider them further.

Different electron microscopic approaches can be used to determine macromolecular weight, but electron microscopy (EM) has not as yet had a prominent position for the determination of molecular weight of polysaccharides unlike for the case of DNA [199]. There are mainly two basically different approaches that can be used. One is based on mixing a specific concentration of the polysaccharide under investigation with a certain amount of another macromolecule with known molecular weight. Provided that the two types of molecules are clearly distinguished by the electron microscope, that they are non-interacting and assuming that they are equally spread on the surface used to prepare the specimen to be observed an average molecular weight can be obtained by counting the two types of molecules in a certain field. To our knowledge, again there are no examples of this approach in the determination of molecular weight of polysaccharides in the literature. The second approach using EM is analogous to a

technique used to determine the molecular weight of DNA. It is based on the principle that if the linear mass density is known, contour length distributions from calibrated electron micrographs can be converted to molecular weight distributions. This technique requires assignment of the whole polymer contour and is therefore limited to rather stiff chains. This application of the electron microscope, together with other applications to carbohydrate polymers, as well as experimental hurdles associated with polysaccharide specimen preparation will be described elsewhere in this volume [200].

Throughout this article light scattering has featured strongly and rightly so—it is arguably the most popular technique for polysaccharide molecular weight determination. It is, however, worth indicating a very simple type of light scattering measurement which as far as we are aware has had no application in polysaccharide molecular weight determination. This is simple turbidity (i.e. *total* intensity loss of an incident beam through scattering). This would be particularly suitable for very large polysaccharides (larger than 10^6 g/mol) providing that Rayleigh–Gans–Debye criteria referred to in Section 4 are still valid. The theory has been worked out, e.g. Doty and Steiner [201], and applied to several viruses, e.g. by Camerini-Otero and Day [202] and Bahls and Bloomfield [203]. Although it is likely to yield only approximate values for polysaccharides, the instrumentation is simple compared to SLS, dynamic light scattering and sedimentation methods: a good quality spectrophotometer (with the proviso that appreciable amounts of low angle *scattered* radiation are not detected) can be used.

10. CONCLUSIONS

As stressed at the start of this article, polysaccharides are characterized by large deviations from ideal behaviour in the thermodynamic sense due to expanded or asymmetric conformations compared to globular proteins, often due to single or multistranded stiff chains and/or high linear charge densities. In ‘Haug’s triangle’ (Fig. 23), where the three idealized macromolecular conformations are put at the corners of the triangle, the polysaccharides generally behave somewhat intermediate between the randomly coiling and

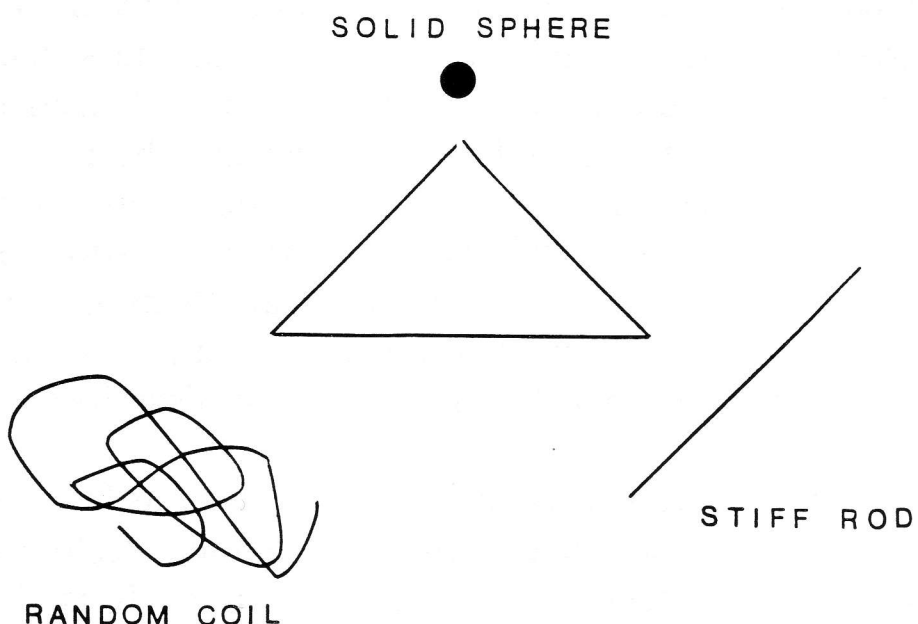


Figure 23. Haug's triangle. The three idealized macromolecular conformations are put at the corners of the triangle.

the stiff rod conformation, and the near ideal behaviour of a polysaccharide is only encountered for the random coil in a θ solvent.

When selecting one particular method for molecular weight determination it is mandatory, as a general rule, to have a general understanding of the conformation to be expected from a knowledge of primary structure. For instance, if rapid measurement of the molecular weight should be sought for by one of the 'relative' methods and the molecule is suspected to have a stiff extended conformation, this would suggest the use of viscometry and not sedimentation transport since the scaling exponent to the molecular weight in these two cases differs by more than a decade (Table 2).

Another problem is that thermodynamic non-ideality (manifested in large second virial coefficients) may be compensated for by a concentration driven aggregation of the macromolecules. Such systems may behave pseudo-ideal in an experiment as a result of two compensating effects. In such cases the use of different experimental methods with different responses to this behaviour is recommended.

Accuracy in molecular weight determination must also be considered critically. The non-ideality in itself may cause large errors in any extrapolation procedure. In addition, the lack of a simple accurate concentration determination technique (Section 2.2) can be the source of rather large uncertainties. Uncertainties in concentration determinations propagate to uncertainties in the determined molecular weight in addition to the measured physical quantity (osmotic pressure, scattered light). This means that molecular weights of polysaccharides can rarely be determined to a higher precision than 5–10% relative uncertainty. This is in contrast to proteins and DNA whose molecular weights can be determined precisely from their primary sequence.

When looking ahead, what are the improvements to be foreseen in the near future? For protein characterization the advent of the SDS-gel electrophoresis system has made possible rather accurate molecular weight determinations with minute sample requirements. Are any such developments to be expected in the polysaccharide field? The first answer is no. A polydisperse macromolecular population cannot be determined and described with the same simplicity as the monodisperse proteins. The on-line techniques (Section 8), where molecular weight separations and molecular weight determinations are performed in sequence, promise a future with more of a routine approach to the present difficult molecular weight, molecular weight averages and distribution determinations of polysaccharides.

ACKNOWLEDGMENTS

We would like to thank our colleagues for their help and encouragement during the writing of this article, in particular Dr J. R. Mitchell. We would also like to thank Dr P. J. Wyatt, Ms K. Jumel and Ms A. Martinsen for permission to use material prior to publication. The support of the Norwegian Council for Industrial & Scientific Research, the United Kingdom Agricultural & Food Research Council and the EEC COST 48 program are gratefully acknowledged.

REFERENCES

- [1] Sandford, P. A. and Baird, J., in Aspinall, G. O. (ed.), *The polysaccharides*. Academic Press, New York, 1983, Vol. 2, pp. 411–490.
- [2] Launay, B., Doublier, J. L. and Cuvelier, G., in Mitchell, J. R. and Ledward, D. A. (eds), *Functional properties of Food Macromolecules*, 1986, pp. 1–78.
- [3] Engster, M. and Abraham, R., *Toxicol. Appl. Pharmacol.*, **38** (1976) 265–282.
- [4] Holzwarth, G., *Dev. Ind. Microbiol.*, **26** (1985) 271–280.
- [5] Goddard, P. and Petrak, K., *J. Bioactive Compat. Polym.*, **4** (1989) in press. See also Friend, D. R. and Pangburn, S., *Site Specific Drug Delivery*, **7** (1987) 53–106.
- [6] Duchere, D., Touchard, F. and Peppes, N. A., *Drug Developments and Industrial Pharmacy*, **14** (1988) 283–313. See also Anderson, M. A., Harding, S. E. and Davis, S. S., *Biochem. Soc. Trans.*, **17** (1989), 1101–1102.
- [7] Alderman, D. A., *Int. J. Pharm. Tech. Prod. Mfr.*, **5** (1984) 1–9.
- [8] Chu, B., Gulari, E., Dinapoli, A., Scheerson, R., Robbins, J. B. and Liu, T. Y., in Sattelle, D. B., Lee, W. I., and Ware D. B. (eds). *Biomedical Applications of Laser Light Scattering* Elsevier, Amsterdam, 1982. pp. 3–20.
- [9] Yanaki, T., Ito, W., Tabata, K., Kojima, T., Norisuye, T., Takano, N. and Fujita, H., *Biophys. Chem.*, **17** (1983) 337–342.
- [10] Fung, Y. C., *Biomechanics. Mechanical Properties of Living Tissues*. Springer Verlag, Berlin, 1981.
- [11] Favis, B. D., Yean, W. Q. and Goring, D. A. I., *J. Wood Chem. Technol.*, **4** (1984) 313–320.
- [12] Reid, E. S., European Patent EP 231997, 1987.
- [13] Massouda, D. F., Sercel, F. J. and Graybeal, C. J., *Mod. Paint Coat.*, **70** (1980) 116–118.
- [14] Tanford, C., *Physical Chemistry of Macromolecules*, John Wiley, New York, 1961.
- [15] Scheraga, H. A. and Mandelkern, L., *J. Am. Chem. Soc.*, **75** (1953) 179–184.
- [16] Yang, J. T., in Anfinsen, C. B., Anson, M. L., Bailey, K. and Edsall, J. T. (eds), *Recent Advances in Protein Chemistry*, Academic Press, New York, 1961, Vol. 16, pp. 323–400.
- [17] Gibbons, R. A., in Gottschalk, A. (ed.), *Glycoproteins: Their Composition, Structure and Function*. 1972, pp. 31–157.
- [18] Bradley, T. D., Ball, A., Harding, S. E. and Mitchell, J. R., *Carbohydr. Polym.*, **10** (1989) 205–214.
- [19] Tomka, I. and Vancso, G., in Mitchell, J. (ed.), *Applied Polymer Analysis and Characterization. Recent Developments in Techniques, Instrumentation, Problem Solving*. Hanser, Munich, 1987 pp. 237–276.
- [20] Tombs, M. P. and Peacocke, A. R., *The Osmotic Pressure of Biological Macromolecules*. Clarendon Press, Oxford, 1974.
- [21] van Holde, K. E. *Physical Biochemistry*, 2nd edn. Prentice Hall, New Jersey, 1985, p. 37.

- [22] Laurent, T. C. and Killander, J., *J. Chromatogr.*, **14** (1964) 317.
- [23] Kawahara, K., Ohta, K., Miyamoto, H. and Nakamura, S., *Carbohydr. Polym.*, **4** (1984) 335–356; Sato, T., Norisuye, T. and Fujita, H., *Macromolecules*, **17** (1984) 2696–2700.
- [24] Vårum, K. M. and Smidsrød, O., *Carbohydr. Polym.*, **9** (1988) 103–117.
- [25] Edmond, E., Farquhar, S., Dunstone, J. R. and Ogston, A. G., *Biochem. J.*, **108** (1968) 755–763.
- [26] Muzzarelli, R. A. A., Lough, C. and Emanuelli, M., *Carbohydr. Res.*, **164** (1987) 433–442.
- [27] Chapman, H. D., Chilvers, G. R. and Morris, V. J., *Carbohydr. Polym.*, **7** (1987) 449–460; Wik, K. O., *PhD Dissertation*, Uppsala University, Sweden, 1979.
- [28] Berth, G., Dautzenberg, H., Lexow, D. and Rother, D., *Carbohydr. Polym.*, **12** (1990) 39.
- [29] Lecacheux, D., Mustiere, Y., Panaras, R. and Brigand, G., *Carbohydr. Polym.*, **6** (1986) 477–492.
- [30] Yanaki, T., Kojima, T. and Norisuye, T., *Polym. J.*, **13** (1981) 1135–1143.
- [31] Wedlock, D. J., Badruddin, B. A. and Phillips, G. O., *Int. J. Biol. Macromol.*, **8** (1986) 57–61.
- [32] Dubois, M., Gilles, K. A., Hamilton, J. K., Rebers, P. A. and Smith, F., *Anal. Chem.*, **28** (1956) 350–356.
- [33] Alexandrovicz, Z., *J. Polym. Sci.*, **40** (1959) 91.
- [34] Eisenberg, H., *Biological Macromolecules and Polyelectrolytes in Solution*, Clarendon Press, Oxford, (1976).
- [35] Oosawa, F., *Polyelectrolytes*, Marcel Decker, New York, 1971.
- [36] Manning, G. S., *Q. Rev. Biophys.*, **11** (1977) 179–246.
- [37] Donnan, F. G., *Z. Electrochem.*, **17** (1911) 572.
- [38] Fishman, M. L., Pepper, L., Dammert, W. C., Phillips, J. G. and Barford, R. A., in Fishman, M. L. and Jen, J. J. (eds), *Chemistry and Functions of Pectins*. ACS Symp. Ser., Washington D.C., 1986 pp. 22–37.
- [39] Smidsrød, O. and Grasdalen, H., *Hydrobiologia*, **116/117** (1984) 19–28.
- [40] Paradossi, G. and Brant, D. A., *Macromolecules*, **15** (1982) 874–879.
- [41] Cleland, R. L. and Wang, J. L., *Biopolymers*, **9** (1970) 799–810.
- [42] Buliga, G. S. and Brant, D. A., *Int. J. Biol. Macromol.*, **9** (1987) 71–76.
- [43] Strutt, J. W. (Lord Rayleigh), *Phil. Mag.*, **41** (1871) 107.
- [44] Kratochvil, P., *Classical Light Scattering from Polymer Solutions*. Elsevier, Amsterdam, 1987.
- [45] Huglin, M. B., In Huglin, M. B. (ed.), *Light scattering from Polymer Solutions*. Academic Press, London, 1972, pp. 163–331.
- [46] Debye, P., *J. Phys. Coll. Chem.*, **51** (1947) 18–32.
- [47] Zimm, B. H., *J. Chem. Phys.*, **16** (1948) 1099–1116.
- [48] Smidsrød, O. and Haug, A., *Acta Chem. Scand.*, **22** (1968) 797.
- [49] Nagasawa, M. and Takahashi, A., in Huglin, M. B. (ed.), *Light Scattering from Polymer Solutions*. Academic Press, London, 1972, pp. 671–723.
- [50] Cossere, E. F. and Eisenberg, H., *J. Phys. Chem.*, **65** (1961) 427.
- [51] Schurr, J. M. and Schmitz, K. S., *Ann. Rev. Phys. Chem.*, **37** (1986) 271–305.

- [52] Flory, P. J., *Statistical Mechanics of Chain Molecules*. John Wiley, New York, 1969.
- [53] Tabor, B. E., in Huglin, M. B. (ed.), *Light Scattering from Polymer solutions*. Academic Press, London, 1972, pp. 2-25.
- [54] Vreeman, H. J., Snoeren, T. H. M. and Payens, T. A. J., *Biopolymers*, **19** (1980) 1357-1374.
- [55] Gulari, E., Chu, B. and Liu, T. Y., *Biopolymers*, **18** (1979) 2943-2961.
- [56] Kashiwagi, Y., Norisuye, T. and Fujita, H., *Macromolecules*, **14** (1981) 1220-1225.
- [57] Coviello, T., Kajiwara, K., Burchard, W., Dentini, M. and Crescenzi, V., *Macromolecules*, **19** (1986) 2826-2831.
- [58] Schachman, H. K., *Nature*, **341** (1989) 259-260.
- [59] Schachman, H. K., *Ultracentrifugation in Biochemistry*, Academic Press, New York, 1959.
- [60] Williams, J. W. (ed.), *Ultracentrifugal Analysis in Theory and Experiment*. Academic Press, New York, 1963.
- [61] Williams, J. W., *Ultracentrifugation of Macromolecules: Modern Topics*. Academic Press, New York, 1972.
- [62] Fujita, H., *Mathematical Theory of Sedimentation Analysis*. Academic Press, New York, 1962.
- [63] Fujita, H., *Foundations of Ultracentrifuge Analysis*. John Wiley, New York, 1975.
- [64] Williams, J. W., Van Holde, K. E., Baldwin, R. L. and Fujita, H., *Chem. Rev.*, **58** (1958) 715-806.
- [65] Van Holde, K. E., in Neurath, H. and Hill, R. (eds), *The Proteins*, 3rd edn. Academic Press, New York, 1975, Vol. 1, p. 228.
- [66] Creeth, J. M. and Pain, R. H., *Prog. Biophys. Mol. Biol.*, **17** (1967) 217-287.
- [67] Teller, D. C., *Methods Enzymol.*, **27** (1973) 371-390.
- [68] Lloyd, P. H., *Optical Methods in Ultracentrifugation Electrophoresis and Diffusion*. Oxford University Press, Oxford, 1974.
- [69] Bowen, T. J. and Rowe, A. J., *An Introduction to Ultracentrifugation*. Wiley-Interscience, London, 1970.
- [70] Creeth, J. M. and Harding, S. E., *J. Biochem. Biophys. Methods*, **7** (1982) 25-34.
- [71] Yphantis, D. A., *Biochemistry*, **3** (1964) 297-317.
- [72] Wales, M., Adler, F. T. and Van Holde, K. E., *J. Phys. Coll. Chem.*, **55** (1951) 145-161.
- [73] Creeth, J. M. and Knight, C. G., *Chem. Soc. Spec. Publ.*, **23** (1968) 303-313.
- [74] Teller, D. C., Horbett, T. A., Richards, E. G. and Schachman, H. K., *Ann. NY Acad. Sci.*, **164** (1969) 66-101.
- [75] Ross, P. D. and Minton, A. P., *J. Mol. Biol.*, **112** (1977) 437-452.
- [76] Harding, S. E. and Johnson, P., *Biochem. J.*, **231** (1985) 543-547.
- [77] Suzuki, H., in Ranby, B. (ed.), *Physical Chemistry of Colloids and Macromolecules*. Blackwell Scientific, Oxford, 1987, pp. 101-109.
- [78] Yphantis, D. A., *Biochemistry*, **3** (1964) 297-317.
- [79] Roark, D. E. and Yphantis, D. A., *Ann. NY Acad. Sci.*, **164** (1969) 245-278.
- [80] Harding, S. E., *Biochem. J.*, **219** (1984) 1061-1064.

- [81] Creeth, J. M. and Cooper, B., *Biochem. Soc. Trans.*, **12** (1984) 618–621.
- [82] Teller, D. C., PhD Dissertation, University of California, Berkley, 1965.
- [83] Creeth, J. M. and Harding, S. E., *Biochem. J.*, **205** (1982) 639–641.
- [84] Kim, H., Deonier, R. C. and Williams, J. W., *Chem. Rev.*, **77** (1980) 659–690.
- [85] Harding, S. E., *Biophys. J.*, **47** (1985) 247–250.
- [86] Tindall, S. H. and Aune, K. C., *Anal. Biochem.*, **120** (1982) 71–84.
- [87] Johnson, M. L., Correia, J. J., Yphantis, D. A. and Halvorson, H. R., *Biophys. J.*, **36** (1981) 71–84.
- [88] Williams, R. C., *Anal. Biochem.*, **48** (1972) 164–171.
- [89] Laue, T. M. and Yphantis, D. A., *Biophys. J.*, **25** (1979) 164A.
- [90] Yphantis, D. A., *Methods Enzymol.*, **61** (1979) 3–12.
- [91] Laue, T. M., Yphantis, D. A. and Rhodes, D. G., *Anal. Biochem.*, **143** (1984) 103–112.
- [92] DeRosier, D. J., Munk, P. and Cox, D. J., *Anal. Biochem.*, **50** (1972) 139–153.
- [93] Carlisle, R. M., Patterson, J. I. H. and Roark, D. E., *Anal. Biochem.*, **61** (1974) 248–263.
- [94] Richards, E. G. and Richards, J. G., *Anal. Biochem.*, **62** (1974) 523–530.
- [95] Harding, S. E. and Rowe, A. J., in Tyrer, J. and Reid, G. T. (eds), *Automatic Fringe Analysis*, Open Tech Press, Loughborough, 1987, pp. 187–200.
- [96] Harding, S. E. and Rowe, A. J., *Optics Lasers Eng.*, **8** (1988) 83–96.
- [97] Harding, S. E. and Rowe, A. J., *Biochem. Soc. Trans.*, **15** (1987) 1046–1047.
- [98] Itou, T., Van, K. and Teramoto, A., *J. Appl. Polym. Sci., Appl. Polym. Symp.*, **41** (1985) 35–48.
- [99] Favis, B. D., Yean, W. Q. and Goring, D. A. I., *J. Wood Chem. Technol.*, **4** (1984) 313–320.
- [100] Ball, A., Harding, S. E. and Simpkin, N. J., In Phillips, G. O., Wedlock, D. J. and Williams, P. (eds), *Gums and Stabilizers in the Food Industry*, Vol. 5. IRL Press, Oxford, 1990, pp. 447–450.
- [101] Seymour, G. B. and Harding, S. E., *Biochem. J.*, **245** (1987) 463–466.
- [102] Gaisford, S. E., Harding, S. E., Mitchell, J. R. and Bradley, T. D., *Carbohydr. Polym.*, **6** (1986) 423–442.
- [103] Winwood, R., PhD Dissertation, University of Nottingham, 1986.
- [104] Horton, D., Riley, D. A. and Hansen, P. M. T., *Biopolymers*, **19** (1980) 1801–1814.
- [105] Woodward, J. R., Phillips, D. R. and Fincher, G. B., *Carbohydr. Polym.*, **3** (1983) 143–156.
- [106] Vårum, K., Harding, S. E. and Smidsrød, O., unpublished observations.
- [107] Berth, G., Dautzenberg, H., Lexow, D. and Rother, G., *Carbohydr. Polym.*, **12** (1990) 39.
- [108] Harding, S. E., Berth, G., Ball, A. and Mitchell, J. R., *Carbohydr. Polym.*, **16** (1991) 1–15.
- [109] Kato, T., Okamoto, T., Tokuya, T. and Takahashi, A., *Biopolymers*, **21** (1982) 1623.
- [110] Wyatt, P. J., personal communication, 1989.

- [111] Wyatt Technology Corp. (Santa Barbara USA), Dawn F Application Note, (1988) 7/8/88NO3.
- [112] Edmond, E., Farquhar, S., Dunstone, J. R. and Ogston, A. G., *Biochem. J.*, **108** (1968) 755–763.
- [113] Ball, A., Harding, S. E. and Mitchell, J. R., *Int. J. Biol. Macromol.*, **10** (1988) 259–264.
- [114] Zimm, B. H. and Crothers, D. M., *Proc. Natl. Acad. Sci. USA*, **48** (1962) 905–911.
- [115] Troll, M., Dill, K. A. and Zimm, B. H., *Macromolecules*, **13** (1980) 436–438.
- [116] Whorlow, R. W. *Rheological Techniques*, John Wiley, New York, 1980.
- [117] Ferry, J. D., *Viscoelastic properties of polymers*, 3rd. edn. John Wiley, New York, 1980.
- [118] Bohdanecký, M. and Kovar, J., *Viscosity of Polymer Solutions*. Elsevier, Amsterdam, 1982.
- [119] Lesec, J., Lecacheux, D. and Marot, G., *J. Liq. Chromatogr.*, **11** (1988) 2571–2591.
- [120] Yamakawa, H. and Yoshizaki, T., *Macromolecules*, **13** (1980) 633–643.
- [121] Yamakawa, H. and Yoshizaki, T., *Macromolecules*, **12** (1979) 32–38.
- [122] Bareis, R. E., *Makromol. Chem.*, **182** (1981) 1761–1774.
- [123] Carriere, C. J., *PhD Thesis*, University of Wisconsin, Madison, 1985.
- [124] Smidsrød, O., *Carbohydr. Res.*, **13** (1970) 359–372.
- [125] Tricot, M., *Macromolecules*, **17** (1984) 1698–1704.
- [126] Smidsrød, O., Glover, R. M. and Whittington, S. G., *Carbohydr. Res.*, **27** (1973) 107–118.
- [127] Kuge, T., Kobayashi, K., Kitamura, S. and Tanahashi, H., *Carbohydr. Res.*, **160** (1987) 205–214.
- [128] Yu, L.-P. and Rollings, J. E., *J. Appl. Polym. Sci.*, **35** (1988) 1085–1102.
- [129] Sato, T., Norisuye, T. and Fujita, H., *Macromolecules*, **17** (1984) 2696–2700.
- [130] Smidsrød, O. and Haug, A., *Biopolymers*, **10** (1971) 1213–1227; Fujii, M., Honda, K. and Fujita, H., *Biopolymers*, **12** (1973) 1177–1195.
- [131] Yamakawa, H., *Ann. Rev. Phys. Chem.*, **35** (1984) 23–47.
- [132] Zhang, L., Liu, W., Norisuye, T. and Fujita, H., *Biopolymers*, **26** (1987) 333–341.
- [133] Holzwarth, G., *Carbohydr. Res.*, **66** (1978) 173–186.
- [134] Cleland, R. L., *Biopolymers*, **23** (1984) 647–666.
- [135] Cael, J. J., Cannon, R. E. and Diggs, A. O., *Am. Chem. Soc. Symp. Ser.*, **150** (1981) 44–59.
- [136] Morris, E. R., Rees, D. A. and Welsh, E. J., *J. Mol. Biol.*, **138** (1980) 383–400.
- [137] Rowe, R. C., *Acta Pharm. Suec.*, **19** (1982) 157–160.
- [138] Lecourtier, J. and Chauveteau, G., *Macromolecules*, **17** (1984) 1340–1343.
- [139] Rowe, A. J., *Biopolymers*, **16** (1977) 2595–2611.
- [140] Hascall, V. C. and Sadler, S. W., *J. Biol. Chem.*, **244** (1969) 2384–2396.
- [141] Iso, N., Mizuno, H., Saito, T. and Onda, N., *Bull. Jpn. Soc. Sci. Fish.*, **45** (1979) 1283–1287.
- [142] Cummins, H. Z., Knable, N. and Yeh, Y., *Phys. Rev. Lett.*, **12** (1964) 150.
- [143] Berne, B. J. and Pecora, R., *Dynamic Light Scattering: With Applications to Biology, Chemistry and Physics*. John Wiley, New York, 1976.
- [144] Chu, B., *Laser Light Scattering*. Academic Press, New York, 1974.

- [145] Bloomfield, V. A. and Lim, T. K., *Methods Enzymol.*, **48F** (1978) 415–494.
- [146] Bloomfield, V. A., *Ann. Rev. Biophys. Bioeng.*, **10** (1981) 421–450.
- [147] Schurr, J. M., *Crit. Rev. Biochem.*, **4** (1977) 371–431.
- [148] Sattelle, D. B., Lee, W. I. and Ware, B. R. (eds.) *Biomedical Applications of Laser Light Scattering*. Elsevier, Amsterdam, 1982; in particular Godfrey, R. E., Johnson, P. and Stanley, C. J., pp. 373–389.
- [149] See, e.g. Sanders, A. and Cannell, D. S., in Degiorgio, V., Corti, M. and Giglio, M. (eds), *Light Scattering in Liquids and Macromolecular Solutions*. Plenum, New York, 1980 pp. 173–182.
- [150] Sattelle, D. B. and Ware, B. R., *Laser Light Scattering in Molecular and Cellular Biology*. Academic Press, London, 1989.
- [151] Pusey, P., in Cummins, H. Z. and Pike, E. R. (eds), *Photon Correlation and Light Beating Spectroscopy*. Plenum Press, New York 1974, pp. 387–428.
- [152] Harper, G. S., Comper, W. D. and Preston, B. N., *Biopolymers*, **24** (1985) 2165–2173.
- [153] Sharman, W. R., Richards, E. L. and Malcolm, G. N., *Biopolymers*, **17** (1978) 2817–2833.
- [154] Robinson, G., Ross-Murphy, S. B. and Morris, E. R., *Carbohydr. Res.*, **107** (1982) 17–32.
- [155] Comper, W. D., Preston, B. N. and Davis, P., *J. Phys. Chem.*, **90** (1986) 128–132.
- [156] Hatt, B. W., in Knapman, C. E. H. (ed.), *Developments in Chromatography*, 1st edn. Applied Science Publishers, London, 1978, pp. 157–199.
- [157] Yau, W. W., Kirkland, J. J. and Bly, D. D., *Modern Size-Exclusion Chromatography*. John Wiley, New York, 1979.
- [158] Barth, H. G., *J. Chromatogr. Sci.*, **18** (1980) 409–429.
- [159] Prud'homme, R. K., Froiman, G. and Hoagland, D. A., *Carbohydr. Res.*, **106** (1982) 225–233.
- [160] Hoagland, D. A., Larson, K. A. and Prud'homme, R. K., *Mod. Methods Size Analysis*, **73** (1986) 277–301.
- [161] Corona, A. and Rollings, J. E., *Sep. Sci. Technol.*, **23** (1988) 855–874.
- [162] Yau, W. W., Ginnard, C. R. and Kirkland, J. J., *J. Chromatogr.*, **149** (1978) 465–487.
- [163] Goto, A., Araki, C. and Izumi, I., *Proc. Int. Soc. Citric.*, **2** (1981) 931–934.
- [164] Revilla, G., and Zarra, I., *J. Exp. Bot.*, **38** (1987) 1818–1825.
- [165] Yau, W. W., Stoklosa, H. J. and Bly, D. D., *J. Appl. Polym. Sci.*, **21** (1977) 1911.
- [166] Yau, W. W., Stoklosa, H. J., Ginnard, C. R. and Bly, D. D., *12th Middle Atlantic Regional Meeting, American Chemical Society*, 5–7 April 1978, paper PO13.
- [167] Hamielec, A. E. and Ouano, A. C., *J. Liq. Chromatogr.*, **1** (1978) 111.
- [168] Dubin, P. L. and Principi, J. M., *Div. Polym. Chem., Am. Chem. Soc. Preprints*, **30** (1989) 400–401.
- [169] Terbojevich, M., Cosani, A., Palumbo, M. and Pregnolato, F., *Carbohydr. Res.*, **157** (1986) 269–272.
- [169a] Vårum, K. M., Martinsen, A. and Smidsrød, O., *Food Hydrocoll.* (1991) (in the press).

- [170] Tung, L. H., *J. Appl. Polym. Sci.*, **13** (1969) 775–784.
- [171] Hamielec, A. E. and Ray, W. H., *J. Appl. Polym. Sci.*, **13** (1969) 1317.
- [172] Tung, L. H. and Runyon, J. E., *J. Appl. Polym. Sci.*, **13** (1969) 2397–2409.
- [173] Deckers, H. A., Olieman, C., Rombouts, F. M. and Pilnik, W., *Carbohydr. Polym.*, **6** (1986) 361–378.
- [174] Maxwell, J. C., Letter to P. Tait, 11 December 1867. Reprinted in Knott, *Tait*, 213–214.
- [175] Klein, M. *Am. Sci.*, **58** (1970) 84–97.
- [176] Ekstrøm, L.-G., Kuivinen, J. and Johansson, G., *Carbohydr. Res.*, **116** (1983) 89–94.
- [177] Ekstrøm, L.-G., *Carbohydr. Res.*, **135** (1985) 283–289.
- [178] Hunt, J. A., Young, T. S., Green, D. W. and Willhite, G. P., *SPE Reservoir Eng.*, Aug (1988) 835–841.
- [179] Basedow, M. and Ebert, K. H., *Polym. Sci., Polym. Symp.*, **66** (1979) 101–115.
- [180] Eigner, W.-D., Beck, R. H. F. and Praznik, W., *Carbohydr. Res.*, **180** (1988) 87–95.
- [181] Vijayendran, B. R. and Bone, T., *Carbohydr. Polym.*, **4** (1984) 299–313.
- [182] Yu, L.-P. and Rollings, J. E., *J. Appl. Polym. Sci.*, **33** (1987) 1909–1921.
- [183] Eigner, W.-D., Billiani, J. and Huber, A., *Papier (Darmstadt)*, **41** (1987) 680–684.
- [184] Jumel, K. and White, C. A., in *Scattering Methods in Polymer Science*. Ellis Horwood, Chichester, 1992, in preparation.
- [185] Wyatt, P. J., Jackson, C. and Wyatt, G. K., *American Laboratory*, May (1988).
- [186] Wyatt, P. J., Hicks, D. L., Jackson, C. and Wyatt, G. K., *American Laboratory*, June (1988).
- [187] Oppenheimer, L. and Mourey, T. H., *J. Chromatogr.*, **298** (1984) 217–224.
- [188] Wasteson, A., *Biochim. Biophys. Acta*, **177** (1969) 152–154.
- [189] Wasteson, A., *Biochem. J.*, **122** (1971) 477–485.
- [190] Kaye, W. and Havlik, A. J., *Appl. Optics*, **12** (1973) 541.
- [191] Tinland, B., Mazet, J. and Rinaudo, M., *Makromol. Chem., Rapid Commun.*, **9** (1988) 69–73.
- [192] Odell, J. A. and Keller, A., *J. Polym. Sci., Polym. Phys.*, **24** (1986) 1889–1916.
- [193] Keller, A. and Odell, J. A., *Colloid Polym. Sci.*, **263** (1985) 181–201.
- [194] Farrell, C. J., Keller, A., Miles, M. J. and Pope, D. P., *Polymer*, **21** (1980) 1292–1294.
- [195] Miles, M. J., Tanaka, K. and Keller, A., *Polymer*, **24** (1983) 1081–1088.
- [196] Peiffer, D. G., Kim, M. W. and Lundberg, R. D., *Polymer*, **27** (1986) 493–502.
- [197] Kavenoff, R., Klotz, L. C. and Zimm, B., *Cold Spring Harbor Symp. Quant. Biol.*, **38** (1974) 1.
- [198] Morris, V. J., in Chan, H. W.-S. (ed.), *Biophysical Methods in Food Research*. Blackwell Scientific, Oxford, 1984, pp. 37–102.
- [199] Lang, D., Bujard, H., Wolff, B. and Russell, D., *J. Mol. Biol.*, **23** (1967).
- [200] Stokke, B. T. and Elgsaeter, A., in White, C. A. (ed.), *Advances in Carbohydrate Analysis*, Vol. 1. JAI Press, London, 1991, pp. 195–247.
- [201] Doty, P. and Steiner, R. F., *J. Chem. Phys.*, **18** (1950) 1211–1220.
- [202] Camerini-Otero, R.D. and Day, L.A., *Biopolymers*, **17** (1978) 2241–2249.
- [203] Bahls, D. M. and Bloomfield, V. A., *Biopolymers*, **16** (1977) 2797–2799.